

THE HISTORY

OF

THE HISTORY OF THE UNITED STATES OF AMERICA

AND

THE HISTORY OF THE UNITED STATES OF AMERICA

AND THE HISTORY OF THE UNITED STATES OF AMERICA

(CONTINUED)

THE HISTORY OF THE UNITED STATES

THE HISTORY OF THE UNITED STATES OF AMERICA

THE HISTORY OF THE UNITED STATES OF AMERICA

THE HISTORY OF THE UNITED STATES OF AMERICA



**REPORT  
ON  
THE COOPERATIVE MINERAL EXPLORATION  
IN  
THE PALMEIROPOLIS AREA  
FEDERATIVE REPUBLIC OF BRAZIL**

(PHASE III)

JICA LIBRARY



1072471[4]

18757

**MARCH, 1989**

**JAPAN INTERNATIONAL COOPERATION AGENCY  
METAL MINING AGENCY OF JAPAN**

国際協力事業団

18759

## PREFACE

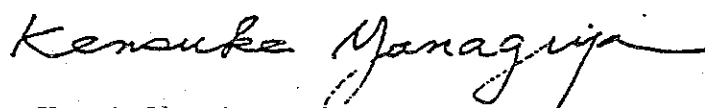
In response to the request of the Government of the Federal Republic of Brazil, the Japanese Government decided to conduct a mineral exploration in the Palmeiropolis area situated in the central part of Brazil, and entrusted the execution of surveys to the Japan International Cooperation Agency (JICA) and the Metal Mining Agency of Japan (MMAJ).

JICA and MMAJ dispatched a four-member survey team to the Federal Republic of Brazil for a period from May 28 to September 17, 1988 to undertake the Phase III Survey as part of exploration project commenced in 1986.

This report, prepared by the survey team after returning to Japan, is a summary of the Phase III Survey conducted in a close cooperation with the officials concerned of the Government of the Federative Republic of Brazil. We trust that this report will serve for the development of the Project, and thereby contribute to the promotion of friendly relation between our two nations.

In submitting this Phase III report, we would like to express our deep appreciation to the officials concerned of the Government of Federal Republic of Brazil for their generous support and cooperation extended to the survey team.

February 1989



Kensuke Yanagiya

President

Japan International Cooperation Agency



Junichi Sato

President

Metal Mining Agency of Japan

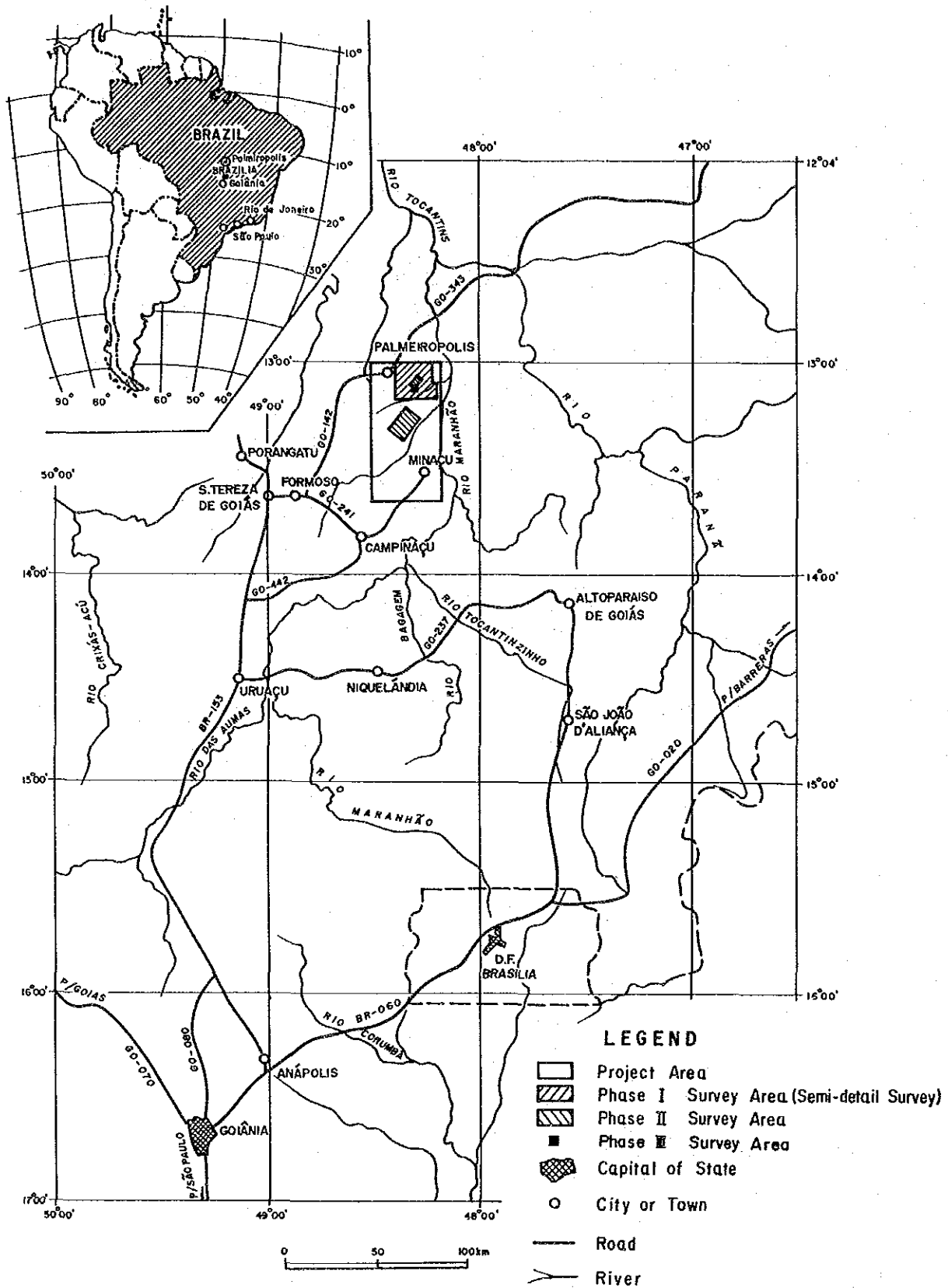


Fig. 1 Location Map of the Project Area

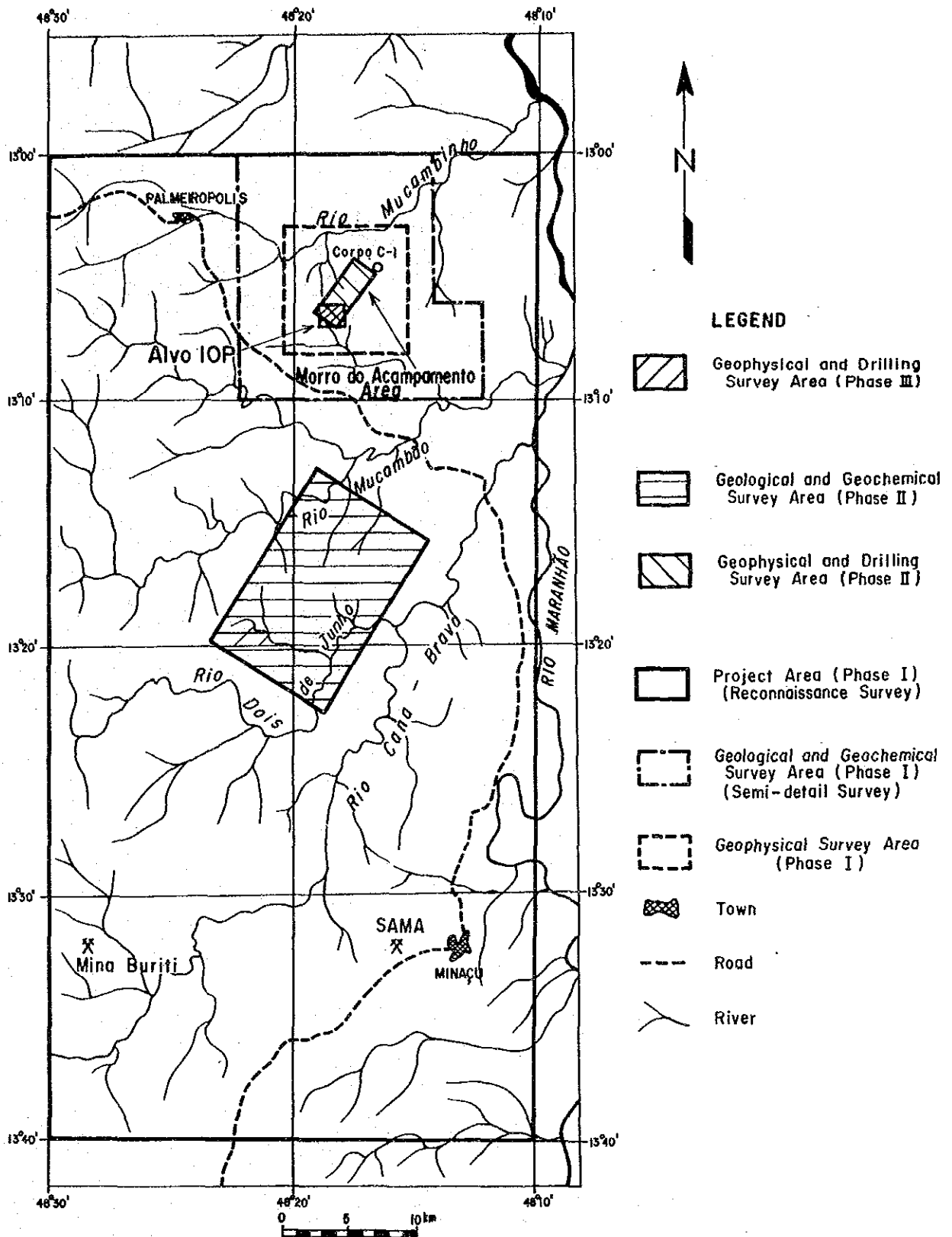
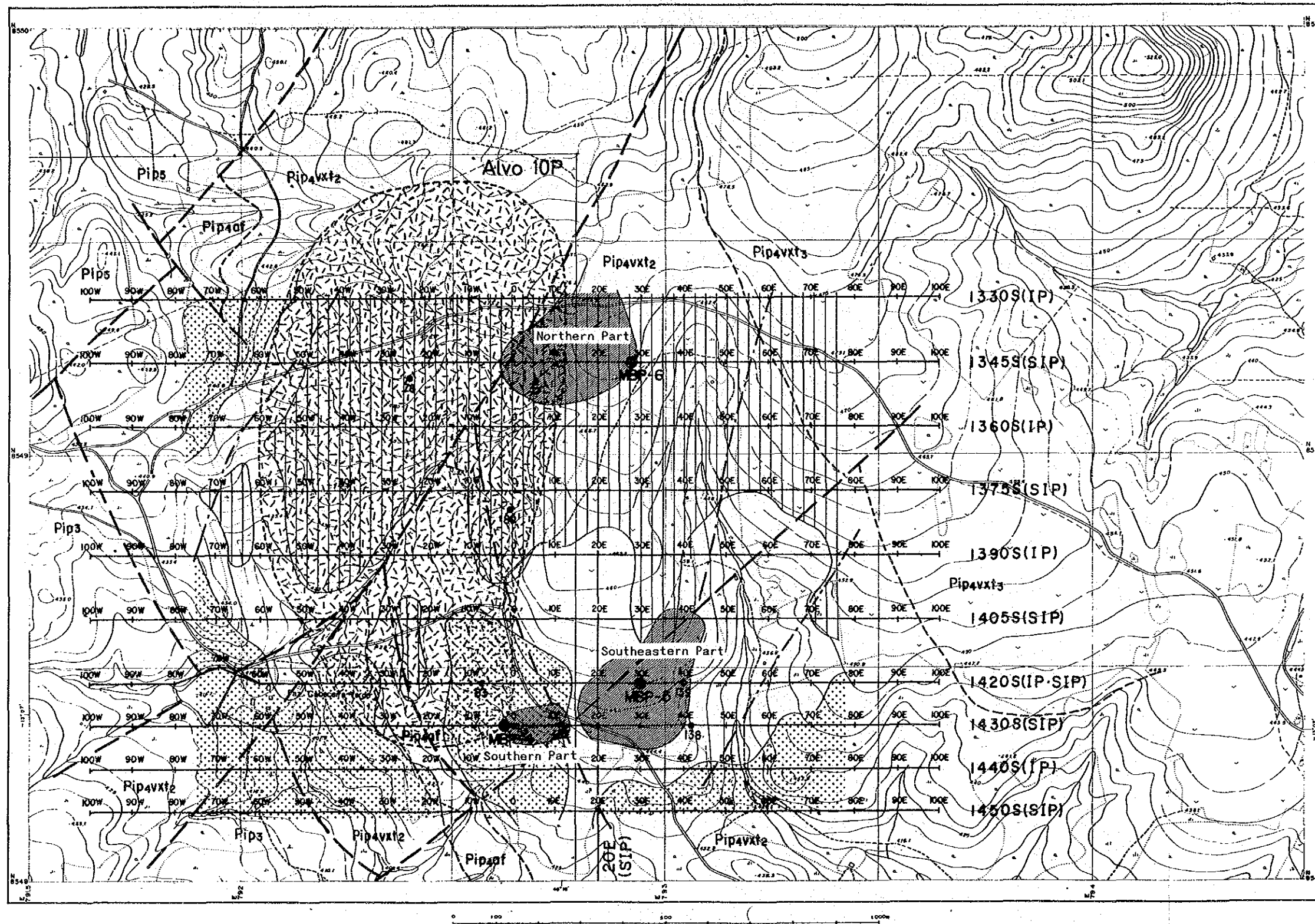


Fig. 2 Location Map of the Surveyed Area



- LEGEND**
- SIP and IP Line
  - Results of Geophysical Survey**
  - $\rho \leq 500 \Omega m$   
(Dep. 200 ~ 300m)
  - $\rho > 1000 \Omega m$   
(Dep. 200 ~ 300m)
  - High IP Anomaly  
(PFE  $\geq 4\%$ )
  - Soil Geochemical Anomaly  
(Pb, Zn)
  - Drilling Point of MMAJ
  - Drilling Point of CPRM
  - Lithologic boundary
  - Fault
  - Tectonic Line Inferred  
by Geophysical Survey

Fig. 3 Summary of Phase III Survey





## ABSTRACT

The current collaborative mineral exploration project in the Palmiropolis area commenced in fiscal year 1986 and continued until fiscal year 1988. This report is a summary of the survey in Phase III, fiscal year 1988, undertaken on the basis of the results obtained in the previous surveys.

The Survey in Phase III included geophysical and drilling surveys conducted in the area centering around Alvo 10P in the Morro do Acampamento area.

From the the geophysical techniques (IP and SIP methods), IP anomalies, presumably correlated to sulfide, were detected at the depths less than 200 meters in the northern, southern and southeastern parts of the said area. The anomalies in the southern and southeastern parts are arranged in a continuous zone which, along with the anomalous zone in the northern part, extends in the direction of NE-SW. The SIP method was useful to discriminate the SIP spectra from some minerals other than pyrite in the southeastern part, however, the method was not able to identify the kind of minerals and occurrences of this anomalous zone. On the other hand, due to the complicated geological structure, the model simulation analysis could not yield a complete information to locate the drill sites.

The drilling surveys were conducted in the above-mentioned three anomalous zones for the MBP-4, MBP-5, and MBP-6 holes for a total length of 1,201.77 meters. The drilling of the MBP-4 hole was executed in parallel with the geophysical surveys. The drilling of the MBP-5 and MBP-6 holes were carried out on the anomalous zones in the southeastern and northern parts of the survey area after the completion of the geophysical surveys.

It was found that the IP anomalous zones detected by the geophysical surveys generally conformed to the mineral dissemination zones identified in the drilling of the MBP-4 and MBP-5 holes. In the MBP-6 hole, however, the exact location of mineralization as the source of the IP anomaly in this particular zone could not be identified.

These mineralization zones belong to two different stratigraphic horizons. The mineralization zone penetrated by the MBP-4 hole is located on a small scale along the boundary between

an amphibolite and a mica schist, both of them in Pip<sub>4</sub>, and is accompanied by massive pyrrhotite. The mineralization zones encountered by all of the drilling holes are emplaced in the mica schist of Pip<sub>4</sub>, and are accompanied by sphalerite, galena and chalcopyrite, with predominant disseminated pyrite. Although these mineralization zones are assumed to be strata-bound deposits, their detection at various and different depths in each drilling hole were due to their complicated folding and faulting structure.

For future exploration, the following surveys are recommended :

1. Detailed surveys in the areas of Alvo 10P, for further evaluation of the mineralization zones determined in the Phase III Survey.
2. Survey to disclose the relationship between the mineralization zone detected in the north of Alvo 10P and the mineralization zone in the South Block detected in the Phase II Survey.
3. Survey program to be applied in this kind of geological background: a) geophysical techniques to reveal geological structures; b) drillings to further clarify the geological structures, c) geophysical techniques to determine mineralization, d) drillings to delineate the mineralization.

## CONTENTS

Preface	
Location Map of the Project Area	
Abstract	

### PART I GENERAL REMARKS

CHAPTER 1	Introduction	1
1-1	Background of the Survey	1
1-2	Conclusion and Recommendation of Phase II Survey	2
1-2-1	Conclusion of Phase II Survey	2
1-2-2	Recommendation of Phase II Survey	2
1-3	Outline of Phase III Survey	3
1-3-1	Survey Area	3
1-3-2	Purpose of the Survey	3
1-3-3	Survey Methods	3
1-3-4	Organization of the Survey Team	4
1-3-5	Period of Investigation	5
CHAPTER 2	Geography of the Survey Area	7
2-1	Topography and Drainage	7
2-2	Climate and Vegetation	8
CHAPTER 3	General Geology	9
CHAPTER 4	Overall Discussion on Survey Results	13
4-1	Geology and Ore Deposits	13
4-2	Results of Geophysical Survey	13
4-3	Results of Drilling	14

CHAPTER 5	Conclusions and Recommendations	17
5-1	Conclusions	17
5-2	Recommendations	17

## PART II PARTICULARS

CHAPTER 1	Outline of the Survey	19
1-1	Field Procedure	19
1-1-1	Geophysical Survey	19
1-1-2	Drilling Survey	25
1-2	Data Processing	25
1-2-1	Geophysical Survey	25
1-2-2	Drilling Survey	27
CHAPTER 2	Survey Results	29
2-1	Results of Geophysical Survey	29
2-1-1	Pseudosections	29
2-1-2	Plan Maps	34
2-1-3	Spectral Diagrams	73
2-1-4	Model Simulation	84
2-2	Drilling Surveys	113
2-2-1	Geology and Mineralization of Hole MBP-4	120
2-2-2	Geology and Mineralization of Hole MBP-5	130
2-2-3	Geology and Mineralization of Hole MBP-6	135
2-3	Discussion	145
2-3-1	Discussion on the Results of Geophysical Survey	145
2-3-2	Discussion on the Results of Drilling Survey	151
2-3-3	Discussion on the detection of a massive ore	157

**PART III CONCLUSIONS AND RECOMMENDATIONS**

Chapter 1 Conclusions .....159  
Chapter 2 Recommendations .....161  
  
REFERENCES .....163  
APPENDICES



## LIST OF FIGURES

Fig. 1	Location Map of Project Area
Fig. 2	Location Map of Survey Area
Fig. 3	Summary of Phase III Survey
Fig. I-3-1	Generalized Stratigraphic Columnar Section in Project Area
Fig. II-1-1	Location Map of SIP-IP Survey and Drilling Holes
Fig. II-2-1	SIP Pseudo-Section (Line-1345S)
Fig. II-2-2	SIP Pseudo-Section (Line-1375S)
Fig. II-2-3	SIP Pseudo-Section (Line-1405S)
Fig. II-2-4	SIP Pseudo-Section (Line-1420S)
Fig. II-2-5	SIP Pseudo-Section (Line-1430S)
Fig. II-2-6	SIP Pseudo-Section (Line-1450S)
Fig. II-2-7	SIP Pseudo-Section (Line-20E)
Fig. II-2-8	IP Pseudo-Section (Line-1330S)
Fig. II-2-9	IP Pseudo-Section (Line-1360S)
Fig. II-2-10	IP Pseudo-Section (Line-1390S)
Fig. II-2-11	IP Pseudo-Section (Line-1420S)
Fig. II-2-12	IP Pseudo-Section (Line-1440S)
Fig. II-2-13	Apparent Resistivity Map [n-spread 1]
Fig. II-2-14	Apparent Resistivity Map [n-spread 3]
Fig. II-2-15	Apparent Resistivity Map [n-spread 5]
Fig. II-2-16	Frequency Effect Map [n-spread 1]
Fig. II-2-17	Frequency Effect Map [n-spread 3]
Fig. II-2-18	Frequency Effect Map [n-spread 5]
Fig. II-2-19	Phase Spectrum Diagram
Fig. II-2-20	Cole-Cole Diagram
Fig. II-2-21	Magnitude Spectrum Diagram
Fig. II-2-22	Cole-Cole Diagram of Three Spectral Types for Rock and Ore Samples
Fig. II-2-23	Location Map of SIP Survey (Phase I, II, III)
Fig. II-2-24	Typical SIP Spectra in the Surveyed Area



Fig. II-2-25(1)	Typical SIP Spectra in Line-1420S
Fig. II-2-25(2)	Typical SIP Spectra in Line-1430S
Fig. II-2-26 (1-2)	2-D Model Calculation (Line-1345S)
Fig. II-2-27 (1-2)	2-D Model Calculation (Line-1420S)
Fig. II-2-28 (1-5)	2-D Model Calculation (Line-1430S)
Fig. II-2-29(1)	Progress Record of MBP-4
Fig. II-2-29(2)	Progress Record of MBP-5
Fig. II-2-29(3)	Progress Record of MBP-6
Fig. II-2-30(1)	Generalized Lithologic Log of MBP-4
Fig. II-2-30(2)	Generalized Lithologic Log of MBP-5
Fig. II-2-30(3)	Generalized Lithologic Log of MBP-6
Fig. II-2-31	Geophysical Interpretation Map
Fig. II-2-32	Geological Profile of MBP-4, MBP-5, and MBP-6

## LIST OF TABLES

Table II-1-1	Geophysical Survey Method
Table II-1-2	Amount of Geophysical Survey
Table II-1-3	Geophysical Survey Instruments
Table II-1-4	Electrical Property of Core Samples
Table II-1-5	Items Analysed and Numbers
Table II-1-6	Flow-chart of Model Analysis for Geophysical Survey
Table II-2-1	Drilling Equipments
Table II-2-2	Drilling Results and Consumed Articles
Table II-2-3	Chemical Assay Data of Drilling Cores

## LIST OF APENDICES

Photo A-1	Microphotograph of Thin Section
Photo A-2	Microphotograph of Polished Section
Table A-1	Microscopic Observations (Thin Section)
Table A-2	Microscopic Observations (Polished Section)
Fig. A-1	Phase Pseudo-Section
Fig. A-2	Spectra of Drilling Cores
Fig. A-3	Lithologic Logs of Drilling Cores (1 : 200)

## LIST OF PLATES

PL. II-1-1	Location Map of SIP-IP Survey and Drilling Holes	(1 : 5000)
PL. II-2-1	SIP Pseudo-Section (Line-1345S)	(1 : 5000)
PL. II-2-2	SIP Pseudo-Section (Line-1375S)	(1 : 5000)
PL. II-2-3	SIP Pseudo-Section (Line-1405S)	(1 : 5000)
PL. II-2-4	SIP Pseudo-Section (Line-1420S)	(1 : 5000)
PL. II-2-5	SIP Pseudo-Section (Line-1430S)	(1 : 5000)
PL. II-2-6	SIP Pseudo-Section (Line-1450S)	(1 : 5000)
PL. II-2-7	SIP Pseudo-Section (Line-20E)	(1 : 5000)
PL. II-2-8	IP Pseudo-Section (Line-1330S)	(1 : 5000)
PL. II-2-9	IP Pseudo-Section (Line-1360S)	(1 : 5000)
PL. II-2-10	IP Pseudo-Section (Line-1390S)	(1 : 5000)
PL. II-2-11	IP Pseudo-Section (Line-1420S)	(1 : 5000)
PL. II-2-12	IP Pseudo-Section (Line-1440S)	(1 : 5000)
PL. II-2-13	Apparent Resistivity Map [n-spread 1]	(1 : 5000)
PL. II-2-14	Apparent Resistivity Map [n-spread 3]	(1 : 5000)
PL. II-2-15	Apparent Resistivity Map [n-spread 5]	(1 : 5000)
PL. II-2-16	Frequency Effect Map [n-spread 1]	(1 : 5000)
PL. II-2-17	Frequency Effect Map [n-spread 3]	(1 : 5000)
PL. II-2-18	Frequency Effect Map [n-spread 5]	(1 : 5000)
PL. II-2-19	Geological Profile for MBP-4, MBP-5 and MBP-6	(1 : 5000)



**PART I GENERAL REMARKS**





## CHAPTER 1 Introduction

### 1-1 Background of the Survey

In the Palmeiropolis area, Palmeiropolis ore deposit is found by CPRM (1975-1984). The ore deposit is composed of three ore bodies and the ore reserves is reported four million tons (Cu 0.46 ~ 1.25%, Pb 0.33 ~ 1.38%, Zn 4.22 ~ 5.85%).

This project started in 1986 with the purpose to determine the possibility of mineral resources in Palmeiropolis area.

In Phase I, fiscal year 1986, a geological reconnaissance survey and a geochemical survey using stream sediments were conducted in the Palmeiropolis entire area. A geological, a soil geochemical and a geophysical survey (CSAMT method) were also conducted in the semi-detailed survey area. As the result of Phase I survey, some zones in Morro do Acampamento Area were regarded as very promising areas and Rio Dois de Junho Area gave indications of being a promising area.

In Phase II, fiscal year 1987, a geophysical survey (SIP method) and a drilling (3 holes) survey were conducted with the purposes to reveal geological structure and to determine the promising areas of mineralization in the areas, northeast and southwest of Morro do Acampamento, where were selected in semi-detailed survey area in Phase I. Geochemical survey was also conducted in Rio Dois de Junho area in Phase II. The results are described in next clause. Mineralization was detected. However, it was not a very good one.

In Phase III, fiscal year 1988, Alvo 10P, located to the south of the Phase II area and covers 3 km<sup>2</sup>, was targeted. In Alvo 10P, the same ore hosting horizon as the one of Palmeiropolis ore deposit is distributed, Cu-Pb-Zn anomalous zone is detected in soil geochemical survey of Phase I and soil geochemical anomalies and IP anomalies were determined by former Brazilian surveys. Drilling conducted by CPRM detected mineralization above 150m of depth. However, information concerning further deep mineralization and structure was needed because it was not enough.

Thus, in order to detect mineralization zones and to investigate the characteristics by obtaining necessary information from the depth concerning the geological structure of the said area, geophysical survey (SIP, IP methods) and drilling survey were conducted.



## 1-2 Conclusions and Recommendations of Phase II Survey

### 1-2-1 Conclusions of Phase II Survey

The target sites for the Phase II Survey are the Rio Dois de Junho and Morro do Acampamento areas.

#### (1) Rio Dois de Junho Area

A geochemical anomalous zone of Cu-Pb-Zn was extracted in the southern part of the area. It seems, however, difficult to expect the existence of any sizable ore deposits of the same type as that of the Palmeiropolis ore deposit, because the zone is very small in scale.

#### (2) Morro do Acampamento Area

The area was divided into two blocks: the North Block and the South Block, and exploration was conducted in each block respectively.

- 1) In the North Block, the MBP-1 hole was drilled to confirm the IP anomalies detected at the depth, around survey point 85W of survey line 150S. No significant mineralization, however, was recognized in this drilling.
- 2) In the South Block, strong IP anomalies having almost the same magnitude as that of the anomalies in the C-1 deposit were detected in a low to medium resistivity zone in the western part of the block. This anomaly zone extends in the south-north direction. In order to confirm the IP anomalies, the MBP-2 and MBP-3 holes were drilled. As a result, dissemination of sulfide minerals at a maximum weight percentage of approximately seven was found for a width of 70-100 meters. The sulfide minerals mainly consisted of pyrite and pyrrhotite, and included graphite-quartz schist therein. Nevertheless, only a small fraction of useful minerals such as chalcopyrite was found in this block.

### 1-2-2 Recommendations of Phase II Survey

It is presumed that the graphite-quartz schist, distributed in the surface of the South Block and determined by drillings, can be correlated to the iron formation overlying the C-1 and C-2 ore deposits located to the north of the Phase II survey area. Therefore, it is considered that the South Block still remains to be explored further for possible ore deposits because the ore hosting horizon same as C-1 and C-2 ore deposits may be present.

Also, in Alvo 10P in the southern edge of the Phase II survey area, both geochemical and IP anomalies had been previously detected by CPRM and the survey of Phase I also detected the geochemical anomaly. 200-meter level drilling conducted by Brazilian side had indicated the possibility of an ore deposit. However, the data obtained in their surveys had been largely confined to those from the shallow part, and thus were insufficient to make a comprehensive evaluation on the Palmeiropolis-type ore deposit.

In order to obtain sufficient information from the depth, therefore, it was recommended that the following follow-up surveys be carried out in the Morro do Acampamento area:

- 1) Conduct drilling for a final evaluation of the South Block.
- 2) Conduct geophysical exploration (SIP) and drilling to obtain necessary information at depths of the Alvo 10P area.

### 1-3 Outline of Phase III Survey

#### 1-3-1 Survey Area

The Phase III Survey covers the Alvo 10P area and its vicinities, in the southern edge of Morro do Acampamento (Fig. 2).

#### 1-3-2 Purpose of the Survey

The purpose of the Phase III Survey is to find areas with possible ore deposits and promising mineralization in the Alvo 10P area, by obtaining necessary information from the depth, and there by examining geological conditions, and analyzing the characteristics of IP anomaly sources within Alvo 10P. In Alvo 10P, a same ore hosting horizon as Palmeiropolis ore deposit is present, geochemical anomalies are detected and mineralization is detected in the shallower by Brazilian side drilling. The area or areas thus extracted are then drilled to confirm the existence of an ore deposit and/or mineralization.

#### 1-3-3 Survey Methods

The IP and SIP electric explorations are conducted, using Dipole-Dipole electrodes placed in the east-west direction, approximately perpendicular to the geological structure of the area,

Ten survey lines are set, and the IP and SIP explorations are conducted alternately. One survey line trending north is also set for the SIP survey.

Data obtained at every survey point were processed and analysed in the camp using a microcomputer. Then two dimensional simulation analysis were adopted for the determination of the source of IP anomalies.

Three drillings (MBP-4, MBP-5, MBP-6) were conducted. The depth of each hole was about 400m. MBP-4 was drilled in the vicinity of PM-52-GO conducted by CPRM simultaneously with the geophysical survey. MBP-5 and MBP-6 were drilled on the IP anomalous source determined by the geophysical survey (Fig. II-2-26 (1) Fig. II-2-27 (1)).

#### 1-3-4 Organization of the Survey Team

The people who participated in the planning and consultation process of the Phase III Survey, and the members of the field survey team are listed below. The field survey team includes two geological engineers from the Brazilian counterpart: one from Departamento Nacional da Produção Mineral (DNPM), and the other from Companhia de Pesquisa de Recursos Minerais (CPRM) commissioned by DNPM.

##### (1) Planning and Consultation Staff

Japanese side:

Kyoichi Koyama, MMAJ

Toshihiko Hayashi, MMAJ

Hideaki Mukai, MMAJ (Rio de Janeiro Office)

Brazilian side:

Jose Belfort dos Santos Bastos, DNPM

Carlos Oiti Berdert, DNPM

Boliver Goncalves Siqueira, DNPM

Walter Hugo Schmaltz, DNPM

##### (2) Field Survey Team

Japanese side:

Kazuo Kawakami, Team Leader, (BEC)

Tomio Tanaka, Geophysicist, (BEC)

Keiji Tanaka, Geophysicist, (BEC)

Kazuto Matsukubo, Geophysicist, (BEC)

Bishmetal Exploration Co., Ltd. (BEC)

Brazilian side:

Homero Lacerda, Team Leader, DNPM

Jose dos Anjos Barreto, Geophysicist, DNPM

**1-3-5 Period of Inverstigation**

**(1) Geophysical survey**

Survey period: May 28, 1988 – February 10, 1989

Field survey: June 5, 1988 – July 10, 1988

**(2) Drilling**

Survey period: May 28, 1988 – February 10, 1989

Fiedl Survey: June 4, 1988 – September 10, 1988

**(3) Report preparation**

July 11, 1988 – February 10, 1989



## CHAPTER 2: GEOGRAPHY OF THE SURVEY AREA

The survey area is located to the east-southeast of the Palmeiropolis settlement of the Municipality of Parana (Parana Municipio) in the central part of the State of Goias.

The survey area can be reached through Municipal Road BR-153 and State Highway GO-080 from Goiania, the capital city of the State of Goias, via Sta. Tereza de Goias. The Morro do Acampamento area is situated approximately 20 km to the east of the Palmeiropolis settlement. The distance between the City of Goiania and the survey area is about 637 km, and it takes 10 hours by car to get to the survey area from the city.

### 2-1 Topography and Drainage

Topography of the survey area is generally flat, and the difference of elevation between the lowest part in the south and the highest part in the north is only 75 meters. In this seemingly flat topography, several small ups and downs associated with the particular geology of the area, nevertheless exist. Generally speaking, the areas where mica schist is distributed have a gentle slope, while the areas where chert is intercalated, exhibit slopes of several tens centimeters because of the chert rocks survived the weathering process and remained comparatively intact. In the areas where canga is present, undulations are still steeper and the highest part reaches up to approximately one meter above the ground surface. In the area to the west of the Phase III drilling site in the southwest of the survey area, elevation reaches up to several meters above the ground surface due to unweathered amphibolite.

From the central to the western parts the survey area, the uppermost streams of Rio Mocambão, a tributary river of Rio Maranhão (the Maranhão River), is running down to the south. The slope is gentle and the stream flow is slack. At the end of each stream, however, soil erosion is apparent, indicating the thickness of top soil and a strong stream flow in the rainy season.

## 2-2 Climate and Vegetation

The survey area belongs to the tropical-humid climate, and the distinction between the rainy and dry seasons is clearly observed. Precipitation and temperature are as follows:

Rainy season: November to March, with precipitation of 1,300-1,800mm

Dry season: April to October

Temperature: Annual average 23-24°C

Maximum 41°C

Minimum 15°C

Vegetation of the survey area exhibits the characteristics of a xerert-savanna type, with thick growths of shrub and grass.

### CHAPTER 3 GENERAL GEOLOGY

The geology of the Palmeiropolis area belongs to the Brazil Central shield from the standpoint of global geologic structure of the South American Continent, and consists of metamorphic and volcanic rocks of the Archaean to Proterozoic.

The Proterozoic in which many metaliferous ore deposits of Brazil are found is widely distributed in Goiás State.

The main known ore deposits emplaced in the Precambrian formations in Goiás State, including the Palmeiropolis area, include Cu-Ni deposits in ultrabasic rock (Niquelandia Deposit and Americano do Brasil Deposit), Asbestos deposit (Cana Brava Deposit), Cu deposit (Mara Rosa Deposit) in basic to acidic volcano-sedimentary metamorphic sequence Cu-Pb-Zn deposit (Palmeiropolis deposit) and Sn-W deposit (Serra da Mesa type) in granitic rocks intruding the above rocks.

The stratigraphy of the Palmeiropolis area is roughly divided into the formations of Archaean and Proterozoic, and the latter is further classified into the lower, middle and upper parts.

The typical stratigraphy of each formation is as follows:

(1) Archaean

Cana Brava basalt-ultrabasic rock massif: granulite-basic to ultrabasic complex, granite-gneiss-migmatite complex

(2) Proterozoic

(a) Lower Proterozoic: Palmeiropolis volcano-sedimentary sequence . . . ultrabasic to basic rocks, schist, granite

(b) Middle Proterozoic: Serra da Mesa Group . . . quartzite, schistose rocks, limestone to marble, basic rocks

Rio Maranhão cataclastic zone . . . quartzite, schistose rocks, gneiss

(c) Upper Proterozoic: Paranoá Group . . . quartzite, dolomite, slate, conglomerate

It has been made clear as the result of exploration by DNPM and CPRM (1983) and CPRM (1984) that the Cu-Pb-Zn deposit in the Palmeiropolis area is emplaced in the Palmeiropolis volcano-sedimentary sequence of the lower Proterozoic.

The Palmeiropolis volcano-sedimentary sequence has been further subdivided by CPRM into three units: Unidade de Oeste (western unit), Unidade de Central (central unit) and Uni-



dade de Leste (eastern unit). The application of this classification is limited to the northern part of the survey area, and the classification by DNPM/CPRM (1983) was more effective for the whole area; that is, the sequence is divided, from the base upward, into Pip<sub>1</sub>, Pip<sub>2</sub>, Pip<sub>3</sub>, Pip<sub>4</sub> and Pip<sub>5</sub>. The palmeiropolis ore deposit is emplaced between Pip<sub>3</sub> and Pip<sub>4</sub> formations.

Geological Unit	Symbol	Columnar Section	Lithology	Geohistory	Metallurgy	Tectono-Magmatic Cycles	Geologic Age
Paraná Group	Ppa		Photo interpretative Unit: quartzite, calcareous and graphitic phyllite, calc-schist, marble and sericite-quartzite	Sedimentation	<ul style="list-style-type: none"> <li>Limestone associated with Pb-Zn-Cu-Ag Showings.</li> <li>Graphite.</li> <li>Magnetite dissemination and Mn supergene Belt.</li> </ul>	Brasiliano Cycle (700-550 m.a.)	Late Proterozoic (1,100-570 m.a.)
Rio Maranhão Crataonic Zone	Ct		<ul style="list-style-type: none"> <li>r: granite intrusive</li> <li>qt: quartzite</li> <li>xt: qtz-mv sch., qtz-sch., bt-mv sch., gnt-mv sch., calc sch. and cl-mv-qtz sch.</li> <li>af: amphibolite intrusion</li> <li>gn: gneiss (basement)</li> </ul>	Cataclastic metamorphism including basement and orogenic belt	Sn and other minerals associated with pegmatite within and around granitic body.		
Serra da Mesa Group (MARINI, 1976)	Pm1		<ul style="list-style-type: none"> <li>qt: mg-bearing sc. quartzite</li> <li>fl: gray phyllite, with mg. in local</li> <li>xt: qtz-cl sch. and cl-qtz sch. with lenticular friable quartzite and graphite sch.</li> <li>mb: basic rock in sch. with mg. (post-metamorphism)</li> <li>cc: marble</li> <li>clt: cl. sch. and foliated quartzite</li> </ul>	Sedimentation with subordinate volcanism. Intrusion of stanniferous granite during orogeny of Serra da Mesa Group.	<ul style="list-style-type: none"> <li>Limestone and graphite. Magnetite dissemination in phyllite.</li> </ul>	Unasquero Cycle (1,200-900 m.a.)	Middle Proterozoic (1,900-1,100 m.a.)
	Pm2m		<p>Photointerpretative Unit:</p> <ul style="list-style-type: none"> <li>r: Serra Dourada and Serra da Mesa Granite</li> <li>Pm2m: graphitic sch., mv-qtz sch., gnt-mv-qtz sch., bt-mv-qtz sch. and quartzite</li> <li>cc: calcareous quartzite</li> </ul>		<ul style="list-style-type: none"> <li>** Barite, limestone and graphite.</li> <li>** So, F, Ta, Nb, beril, tourmaline and muscovite.</li> </ul>		
Piracicaba Volcano-Sedimentary Sequence (RIBEIRO FILHO and TEIXEIRA, 1981)	Pip		<ul style="list-style-type: none"> <li>r: Filo granite</li> <li>S: str-bt-mv-qtz sch., ky-bt-mv-qtz sch., gnt-mv-qtz sch. and ky-str-mv-qtz sch. associated with basic sill and dyke (db), banded iron formation (fl) and quartzite (qt)</li> </ul>	Aluminous pelitic sedimentation	<ul style="list-style-type: none"> <li>Fe in iron formation.</li> <li>Kyanite associated with quartzite along fault.</li> </ul>	Transamazonian Cycle (2,200-1,900 m.a.)	Early Proterozoic (2,600-1,900 m.a.)
			<ul style="list-style-type: none"> <li>4vxt: sc-mc-qtz sch. (rhyolitic composition)</li> <li>4vxt: pl-mc-bt-qtz sch. and pl-bt-qtz sch. intercalated with amphibolite (af) (rhyolite to rhyodacitic composition)</li> <li>4vxt: feldspathic bi-qtz sch., str-gnt-bt-qtz sch., bt-af sch., biotite and cl. rock (dacitic to rhyodacitic composition)</li> <li>4vs: feldspathic gnt-bt-qtz sch. and mica sch. including ky. and acidic meta tuff, with quartzite (qt) and amphibolite (af)</li> </ul>	Volcanism-Sedimentation: acidic-intermediate fissure eruption and "neck" (?). Concentration of base metal and Au.	<ul style="list-style-type: none"> <li>"Stratabound"-type volcanogenic Zn-Cu-Pb massive and disseminated sulfide ore deposits. (Corpo C-1 and Albo 10P)</li> </ul>		
			<ul style="list-style-type: none"> <li>3: dark fine-grained amphibolite with quartzite (qt), ferruginous quartzite (qtfc), gnt-bt-mv-qtz sch. (xt) and basic to ultrabasic dyke (db, ub)</li> <li>r: Morro Solto granite</li> <li>2gr: metagraywacke, metaconglomerate and ultrabasic sill (ub)</li> <li>2vc: acidic to intermediate tuff, lapilli tuff, volcanic breccia and their schist</li> <li>i: gabbroic banded coarse-grained amphibolite</li> </ul>	Basic fissure eruption with volcanoclastics. Sedimentation of graywacke. Intrusion of Morro Solto Granite and basic to ultrabasic rock.	<ul style="list-style-type: none"> <li>Volcanogenic Zn-Cu-Pb massive sulfide mineralization detected by drilling hole of Bililton Metals.</li> <li>Supergene lateritized Ni ore deposit concentrated with ultrabasic "sill" in mine claim of Bililton Metals.</li> </ul>		
Cons Brava Basic-Ultrabasic Massif	Acb		<ul style="list-style-type: none"> <li>mg: metabasalto, metazonite and metabrononite</li> <li>sp: serpentinite</li> <li>px: pyroxenite</li> <li>ub: serpentinite and pyroxenite</li> <li>mb: basic to ultrabasic rock (post-metamorphism)</li> </ul>	Basic-ultrabasic complex.	<ul style="list-style-type: none"> <li>Asbestos mineralization consisting of chrysotile (ct), "Stockwork" type in serpentine - SAMA</li> </ul>	Jequit Cycle 2,600-2,600 m.a.	Archaean 2,600 m.a.

Fig. I-3-1

Generalized Stratigraphic Columnar Section in Project Area



## CHAPTER 4 OVERALL DISCUSSION ON SURVEY RESULTS

### 4-1 Geology and Ore Deposits

Geology of the survey area consists of the Pip<sub>3</sub> and Pip<sub>4</sub> formations of the Palmeiropolis volcano-sedimentary sequence of Lower Proterozoic, and exhibits a highly complicated geological structure due to a fold with NE-SW axis and faults in the directions of NE-SW and NW-SE. In the eastern part of the survey area, mica-quartz schist of the Pip<sub>4</sub> formation is widely distributed. In the western and southwestern parts, amphibolite of the Pip<sub>4</sub> and Pip<sub>3</sub> formations is distributed.

The Pip<sub>4</sub> formation is an important ore-bearing horizon, and all the mineralization zones detected in the survey area, including those detected in the Phase III survey, those detected in CPRM's drilling and the one at PM-138, belong to this formation. Among the three known ore bodies, the C-1, C-2 and C-3 ore deposits, C-1 is a Cu-Pb-Zn ore body embedded in the Pip<sub>4</sub> formation directly above the Pip<sub>3</sub> formation. The C-2 and C-3 deposits are Cu-Pb-Zn ore bodies embedded below the iron formation at the uppermost part of the Pip<sub>4</sub> formation. The mineralization zones detected are of two different types in terms of the stratigraphic horizon to which they belong: One is that considered to belong to the horizon between amphibolite and schist as that of the C-1 ore deposit, and the other to the schist horizon located between the C-1 ore deposit and the C-2 and C-3 deposits.

### 4-2 Results of Geophysical Survey

The resistivity distribution in the survey area generally exhibits NW-SE and NE-SW bound block structures (Fig. II-2-31). In the area around the MBP-4 and PM-137 drilling holes, resistivities of less than 500  $\Omega \cdot m$  are distributed. These resistivities are presumably correlated to a fault structure and an accompanying argillization zone. In the northern and eastern parts of the survey area, resistivities of more than 1,000  $\Omega \cdot m$  are widely distributed. Although both the high resistivity zones and the medium to low resistivity zones are distributed in harmony with the Pip<sub>4</sub> formation and the fault structure respectively, their resistivities are considerably variable. This variance is considered to be due to the differences in the amounts and distribution patterns of quartz and biotite contained in abundance in the Pip<sub>4</sub> formation.

The medium to low resistivity zones are closely associated with the low resistivity zones

(marshland and high erosion areas) in the shallow part of the ground, and to the fault structure and accompanying argillization zone mentioned above. Therefore they do not necessarily indicate the possibility of mineralization. In the drilling explorations conducted at the MBP-4 and PM-137 holes, any medium to low resistivity zones, which are considered to indicate the existence of mineralization, were not identified, either.

Most of the IP anomalies are distributed in the high resistivity areas, forming a high resistivity, high P.F.E. anomaly zone (Fig. II-2-31). The anomalous zones are distributed in the southeastern, southern and northern parts of the survey area respectively. The most promising anomaly area is located in the southeastern part. This anomaly area generally shows a spectral pattern considered to be correlated to the pyrite distributed in the shallow part of the ground. Locally, however, it also exhibits a particular spectral pattern considered to be associated with Cu, Pb and Zn.

The anomalous zones detected in the southeastern, southern and northern parts generally form a sequential anomalous zone, with a similar anomaly source. However, it is presumed that their ore-bearing environments are not necessarily the same because of the fault structures between each anomalous zone. Therefore, it is necessary to conduct structural drillings to investigate in detail the geological structure of each anomaly zone in order to pinpoint exact locations of mineralization.

#### 4-3 Results of Drilling

Three holes were drilled for a total length of 1201.77 meters, taking into consideration the results of the previous surveys and those of the Phase III geophysical exploration.

##### (1) MBP-4 Hole

Drilling was conducted through the  $Pip_4$  formation down to the bottom of the hole from the ground surface. The final depth was 400 meters. Dipping of the formations is less than 30 degrees in general, but it reaches up to around 50 degrees in some parts. Small foldings are locally observed.

Mineralization detected in this hole is of two types. The first type of mineralization (Type 1) is the one which is accompanied by chalcopyrite, galena and sphalerite, etc. with pyrite being predominant, and is embedded in the constituent minerals of the  $Pip_4$  formation such as muscovite, biotite, and quartz schist. The second type of mineralization (Type 2) is the one consisted mainly of pyrrhotite, and is embedded on a small scale along the boundary between the

garnet-plagioclase-biotite-quartz schist of the Pip<sub>4</sub> formation and the amphibolite formation (Pip<sub>4</sub>af). In the former type of mineralization in the MBP-4 hole, the highest mineral content of Zn is 1.2%, and the content for other minerals are quite low as shown in Table II-2-3.

### (2) MBP-5 Hole

Drilling was conducted to the depth of 400.45 meters. Geology of this hole belongs to the Pip<sub>4</sub> formation. In the vicinity of the hole a large scale fold system with is presumed to be present. Weak dissemination of pyrite was observed in the entire drilling hole. At the depths of about 61 meters and between 200 meters and 240 meters, the Type 1 mineralization was detected. In views of the depths of this particular mineralization and its mineral composition, this mineralization is considered to be the source of the anomalies detected in the geophysical exploration. The contents of Cu, Pb and Zn are quite low as shown in Table II-2-3.

### (3) MBP-6 Hole

Drilling was conducted to the depth of 401.32 meters. Geology of this hole belongs to the Pip<sub>4</sub> formation. A large scale fold with the fold axis trending NE to NNE is also presumed to exist near this drilling hole. Weak and intermittent dissemination of pyrite was detected in the entire drilling hole, accompanied by a small amount of sphalerite at the depth below 369 meters. Mineral content are very small as shown in Table II-2-3.

As discussed above, a low grade Cu-Pb-Zn mineralization (Type 1) was detected in the Pip<sub>4</sub> formation in all the three drilling holes. The drilling of PM-138-GO conducted by CPRM in the IP anomalous zone detected in the Phase III during geophysical exploration also disclosed the existence of a high grade Cu-Pb-Zn mineralization, which partly forms a massive ore deposit, for a core length of 12 meters in the Pip<sub>4</sub> formation. IP anomalous zones were disclosed as dissemination zones, composed mainly of pyrite accompanied by massive sulfide deposit, by drillings carried out by CPRM and MMAJ. The mineralization zones penetrated by the drillings are presumed to be stratigraphically the same since the ore mineral composition and the occurrences of the mineralizations are similar to each other, host rocks of the mineralization are all mica schist of Pip<sub>4</sub> and three anomalous zones are thought to be continuous from the geophysical point of view. When compared stratigraphically with the C-1, C-2 and C-3 deposits located to the northeast of the survey area, it is presumed that the Type 1 mineralization is located above the C-1 deposit and below the C-2 and C-3 deposits. Type 2 mineralization is presumed to be

stratigraphically located above C-1 ore deposit and below Type 1 mineralization.

It is presumed that a folding structure similar to the overturned folding with an axis extending toward the southwest direction from the vicinity of the C-1 deposit, may exist in the vicinity of the MBP-6 drilling hole. It is therefore presumed that the mineralization discussed above may be located in the Pip<sub>4</sub> formation which, in turn, might have been moved to the present location by the folding movement. This assumption will explain the apparent difference in the depths of mineralization detected in the three drilling holes.

## CHAPTER 5 CONCLUSIONS AND RECOMMENDATIONS

### 5-1 Conclusions

In the Phase III survey, mineralization zones consisted mainly of disseminated pyrite were detected in three locations with IP anomalies in the southwestern part of the Morro do Acampamento area. The drilling conducted by CPRM also confirmed the presence of a massive Cu-Pb-Zn deposit in one of the three locations. These mineralization zones consisted mainly of disseminated pyrite and massive ore deposit are considered to constitute a series. This large mineralized zone should be surveyed more in detail, because some other massive ore deposits are likely to be found.

Geophysical surveys (SIP, IP methods) are effective to determine the presence of mineralization even in this kind of geological background. However, it is thought that geological structure is a very important factor to analyse the data gained, because the shape of ore deposit is controlled by the geological structure. Revealmment of the geological structure should be preceded to the geophysical survey to delineate the mineralization.

### 5-2 Recommendations

The areas including IP anomalous zones should be evaluated by the surveys to reveal the geological background of the mineralization and the presence of other massive ore bodies, and to determine the scales of ore body and the reserves intersected by drilling of CPRM.

For this purpose, therefore, the following activities are recommended:

(1) Re-examination of the geological structure of the Alvo 10P area, using the existing drilling data including those obtained in the Phase III Survey. This includes, in particular, a three-dimensional examination of the known ore deposits through the analysis of the fold structure therein. The shape of ore bodies are thought to be controlled by the fold, which are supposed to have northeast trending axes and southeast dipping axial planes in this area. Therefore, the drillings with a northwest inclination should be conducted and the sites should be aranged along a northeast direction.

(2) Stratigraphic analysis of the Alvo 10P area, using the existing drilling data including those obtained in the Phase III Survey. This includes, in particular, the investigation of stratigraphic order and mineralization environment, with close reference to petrology and mineralogy.



(3) Analysis of the genetic and stratigraphic relationship between the mineralization zone in the South Block detected in the Phase II Survey and the anomaly zone detected in the northern part of the Phase III survey area.

(4) A survey program should be sequentially conducted as follows: a) Revealmnt of geological structure by geophysical techniques, b) Revealmnt of geological structure by drillings, c) Determination of mineralization zone by geophysical techniques, d) Delineation of mineralization by drillings.



**PART II PARTICULARS**





## CHAPTER 1 OUTLINE OF THE SURVEY

In Alvo 10P, which comprises the most part of the Phase III survey area, Pb and Zn anomalies were detected in the geochemical survey of Phase I. These anomalies had been previously detected in the geochemical and geophysical (IP) surveys conducted by CPRM. Their drilling survey had also disclosed the existence of a Pb-Zn mineralization zone at a depth around 100 meters below the ground. However, since their survey had been confined to the depths less than 150 meters, no information as to further depths was available. Accordingly, further surveys to obtain the necessary information from the depth were called for to make a comprehensive evaluation of the target area.

The purposes of the Phase III Survey were to examine spectral characteristics of the known mineralization zones, to detect IP anomalies at the depth by conducting geophysical surveys (IP and SIP), and to make an indepth investigation into the mineralization conditions of the expected Cu-Pb-Zn ore deposits through drilling surveys.

### 1-1 Field Procedure

#### 1-1-1 Geophysical Survey

Discrete frequency signals were sent to the underground from a pair of current electrodes, and return signals were received at another pair of electrodes. Two different frequency signals were sent in the IP method, and 18 different frequency signals were sent in the SIP method.

The return signals varied in accordance with the underground conditions, and phase lag was observed in the return signals when a conductive zone was distributed underneath. By measuring this phase lag, the strength and distribution pattern of anomalies were estimated. In the SIP method, anomalies can be detected precisely because a number of different frequencies are used. The information obtained thereby can be used to differentiate minerals and ore deposits through spectral analysis.

Survey lines were set with the PM-52-GO hole as the base point, after conducting a preliminary survey. Survey points were set at intervals of 50 meters, from the base point of 00. As to the survey lines in which the SIP surveys were conducted, signal lines were set in parallel with the survey lines. Table II-1-1 shows the survey methods and the frequencies used in the SIP and IP electric explorations.

Table II-1-1 Geophysical Survey Method

	SIP Method	IP Method
Measured Frequencies	0.125, 0.375, 0.625, 0.875, 1.0, 1.125, 3, 5, 7, 8, 9, 24, 40, 56, 72Hz	0.3, 3Hz
Electrode Configuration	Dipole-Dipole	Dipole-Dipole

(1) Extent of Geophysical Survey

Table II-1-2 shows the extent of the geophysical survey. The locations of survey lines are shown in Figure II-1-1.

Table II-1-2 Amount of Geophysical Survey

	SIP Method	IP Method
Line Length	2.0 km × 5 Lines 1.8 km × 1 Line 1.6 km × 1 Line	2.0 km × 5 Lines
Measuring Points	488 point	400 point
Line Name	1345S, 1375S, 1405S, 1420S, 1430S, 1450S, 20E	1330S, 1360S, 1390S, 1420S, 1440S





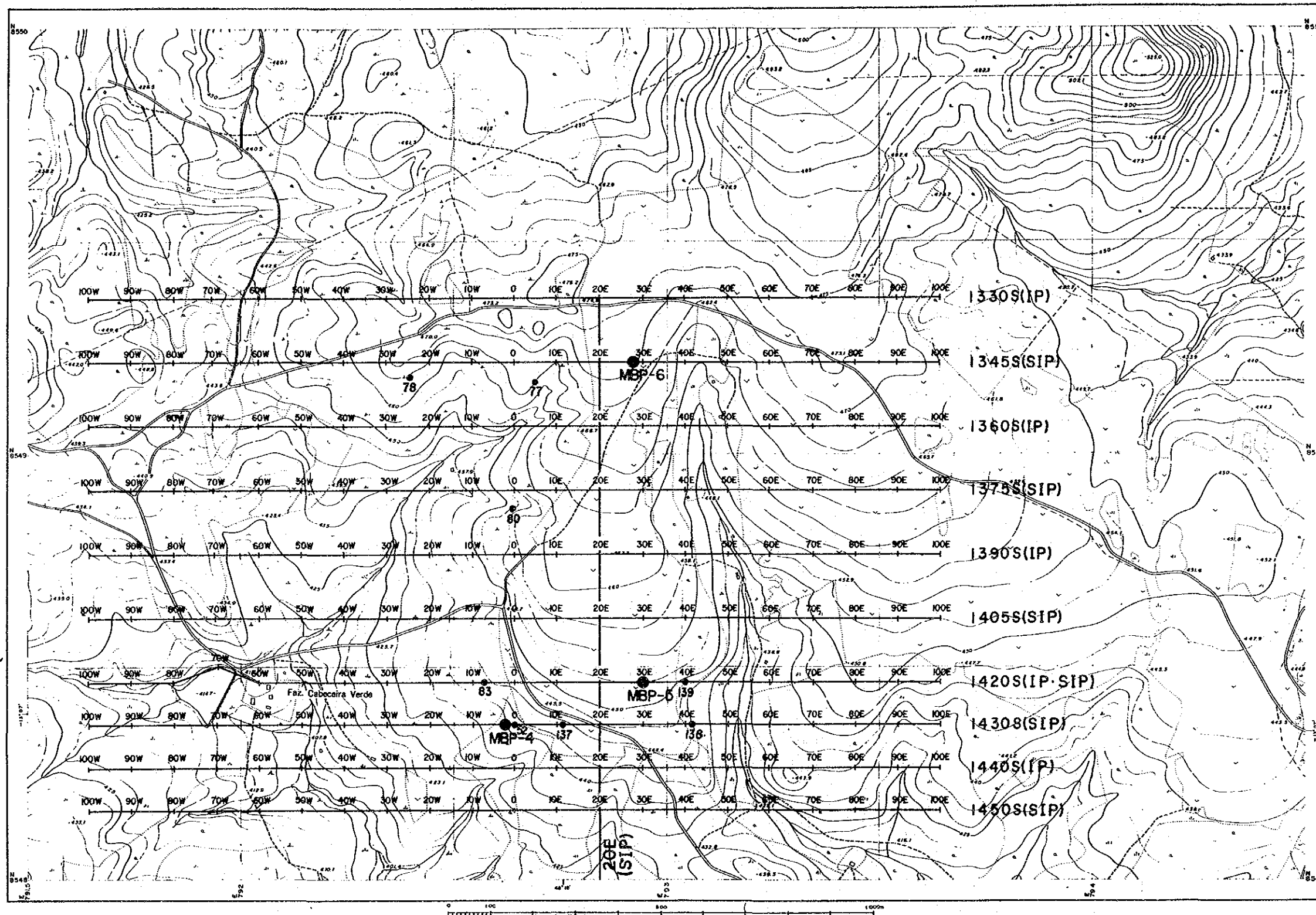


Fig. II-1-1 Location Map of SIP-IP Survey and Drilling Holes

- LEGEND**
- SIP and IP Line
  - Drilling Point of MMAJ
  - Drilling Point of CPRM



## (2) Instruments and Equipment

Table II-1-3 is a list of major instruments and equipment used in this survey.

Table II-1-3 Geophysical Survey Instruments

	SIP Method	IP Method
Transmitting Part	Transmitter GGT-5 SIP Frequency Generator (Model CH-86A) Motor Generator (G400)	Motor Generator (G400)
Receiving Part	Multi-Function Receiver (GDP-12/2GB, GDP-16/8) Data Recorder (DR-1) Isolation Amp (ISO/1)	IP Receiver (Model CH-R7802)

## (3) Rock Property Tests

Laboratory electrical property tests of rock samples were conducted to investigate the properties of the rocks distributed in the survey area. Twenty-six samples were taken from the drilling cores. Table II-1-4 shows the sampling points and test results. In the table, resistivity and raw phase values were determined from the frequency of 0.125Hz, and PFE values from the frequency of 0.125Hz-1.0Hz.

As shown in the table, the average resistivity of the 26 samples is 10,800  $\Omega \cdot m$ , and the average P.F.E value is 4.0%. The respective values in each hole are 12,900  $\Omega \cdot m$  and 4.2% in MBP-4; 5,840  $\Omega \cdot m$  and 3.3% in MBP-5; and 8,550  $\Omega \cdot m$  and 4.0% in MBP-6.

Lithologically, almost ninety percent of the core samples consisted of schist, and amphibolite was observed only in three samples. The average resistivity of the three samples containing amphibolite is 8,700  $\Omega \cdot m$ , with an average P.F.E value of 2.8%.

The resistivity values of the 26 samples generally fall within the range of 4,000  $\Omega \cdot m$  to 12,000  $\Omega \cdot m$ . Exception of this is the values of the samples taken from the shallow part of MBP-4. The low resistivity values of these core samples are considered to reflect the influence of weathering and alteration.

The P.F.E values vary from 1.0% to a maximum of 11.7%, but this variation does not necessarily correspond to the amounts of pyrite observed megascopically. The P.F.E values, therefore, are likely to correspond to the amounts of pyrite particles which are not visible to the naked eye.

Table II-1-4 Electrical Property of Core Samples

Depth of Samples (m)	Resistivity (ohm-m)	Raw Phase (-mrad)	P.F.E. (%)	Lithology	Amount of Sulfide (Pyrite)
MBP-4 16.80 - 16.85	1,030	12.3	1.9	Ms-Qt schist	
MBP-4 24.40 - 24.45	720	24.6	3.8	Ms-Bi-Qt schist	○
MBP-4 42.90 - 42.95	6,270	81.4	11.7	Bi-Ms-Qt schist	⊙
MBP-4 46.70 - 46.75	12,410	24.2	4.2	Bi-Ms-Qt schist	●
MBP-4 85.90 - 85.95	12,560	17.9	2.4	Pl-Bi-Qt schist	○
MBP-4 90.40 - 90.45	11,080	16.7	2.4	Am-Bi-Qt schist	
MBP-4 121.40 - 121.45	4,300	8.7	1.3	Pl-Gn-Bi-Qt schist	
MBP-4 163.95 - 164.00	18,000	20.5	3.0	Pl-Bi-Qt schist	
MBP-4 203.70 - 203.75	35,100	32.9	4.8	Gn-Ms-Bi-Qt schist	
MBP-4 245.20 - 245.25	43,500	61.6	11.5	Gn-Pl-Bi-Qt schist	●
MBP-4 286.40 - 286.45	3,280	18.3	2.6	Gn-Pl-Bi-Qt schist	●
MBP-4 295.45 - 295.50	9,490	27.4	4.7	amphibolite	
MBP-4 313.80 - 313.85	12,480	21.2	3.5	Bi-Qt schist	
MBP-4 348.10 - 348.15	9,500	17.0	2.7	amphibolite	●
MBP-4 358.35 - 358.40	8,060	16.0	2.3	Gn-Ms-Bi-Qt schist	
MBP-4 381.10 - 381.15	19,000	22.8	3.1	Bi-Qt schist	●
MBP-5 79.55 - 79.60	5,900	11.5	1.6	(Ms-Bi)-Qt schist	
MBP-5 120.90 - 120.95	7,580	30.9	3.6	Pl-Bi-Qt schist	●
MBP-5 217.95 - 218.00	2,710	59.1	7.1	Ms-Bi-Qt schist	○
MBP-5 249.65 - 249.70	7,160	6.1	1.0	amphibolite	●
MBP-6 72.95 - 73.00	11,360	35.1	4.8	Pl-(Bi-Ms)-Qt schist	○
MBP-6 155.10 - 155.15	6,150	22.1	3.0	Gn-(Ms-Bi)-Qt schist	
MBP-6 200.05 - 200.10	5,200	17.7	2.6	Gn-(Ms-Bi)-Qt schist	
MBP-6 218.95 - 219.00	4,300	12.7	1.8	Ms-Bi-Qt schist	○
MBP-6 250.00 - 250.05	19,130	47.7	7.6	Pl-Gn-Ms-Bi-Qt schist	●
MBP-6 387.45 - 387.50	5,120	30.4	4.0	Gn-Ms-Bi-Qt schist	○

Relative amount of sulfide determined by naked eye. ● < ○ < ⊙

### 1-1-2 Drilling Survey

Three holes (MBP-4, MBP-5 and MBP-6) were drilled for a total length of 1,201.77 meters. Items and amount of the tests on the above studies are shown in Table II-1-5.

The MBP-4 hole was drilled in the geochemical anomalous zone in the area 25 meters to the west of the CPRM's drilling site (PM-52-GO) where mineralization had already been detected. The primary purpose of the drilling was to make a follow-up study of the known mineralization zone, by obtaining necessary information from the depth for a comprehensive evaluation of the nature and extent of the mineralization. At the same time, it was further purposed to make a comparative study of the geological data to be obtained from the MBP-4 drilling hole and the geophysical data to be obtained in the geophysical exploration in the vicinity of the drilling hole, in order to select the most appropriate drilling sites for MBP-5 and MBP-6.

The MBP-5 and MBP-6 holes were drilled in the areas in which IP anomalies were detected in the geophysical survey of Phase III. The SIP spectral analysis also indicated that these drilling sites had a high possibility of Cu-Pb-Zn mineralization.

Table II-1-5 Electrical Property of Core Samples

Items Analyzed	Number
Thin Section	10
polished Section	6
Chemical Assay (ore)	60
Au, Ag, Cu, Pb, Zn, S'	(360 elements)

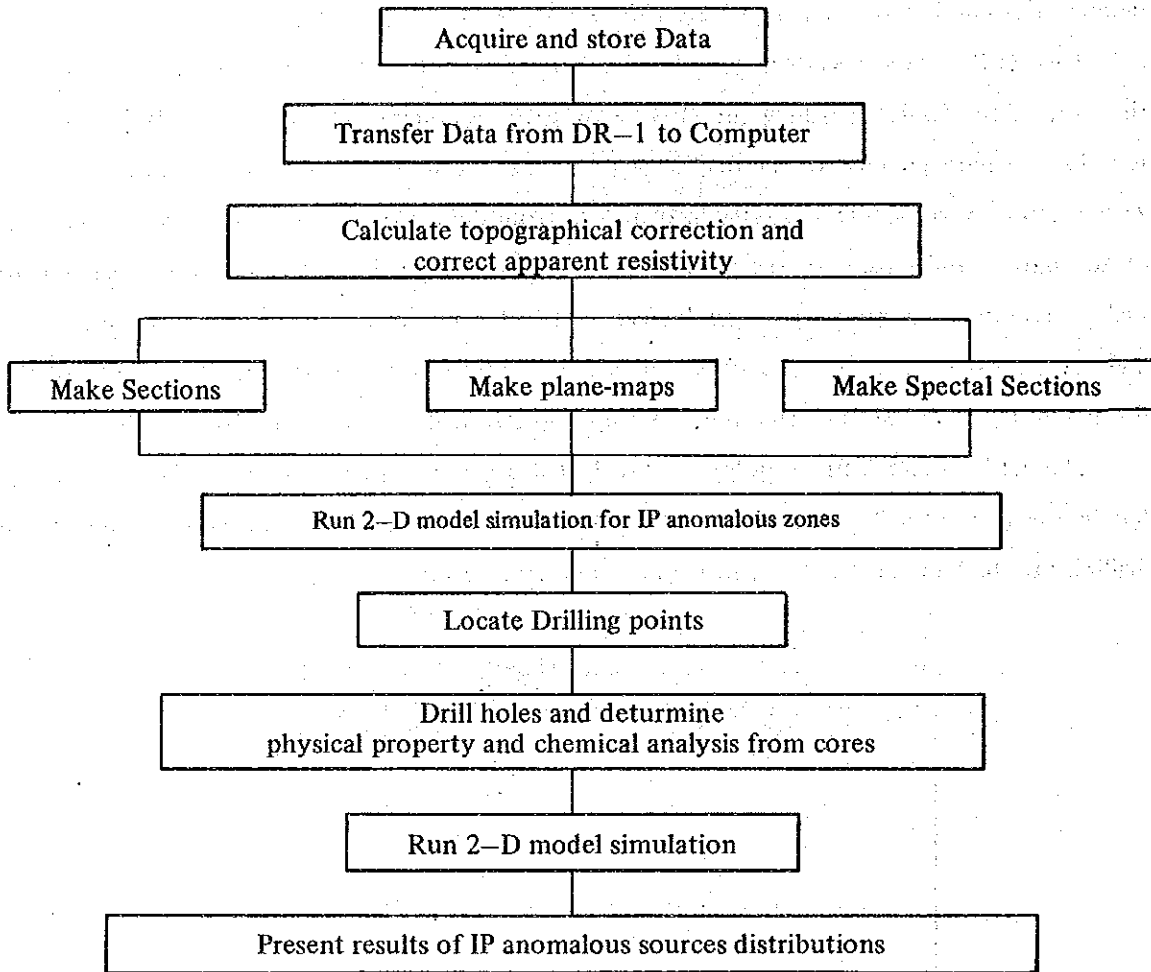
### 1-2 Data Processing

#### 1-2-1 Geophysical Survey

Real-time data processing was made to calculate apparent resistivities, phase differences, spectral patterns, and P.F.E values, and the data thus processed were stored in a data recorder. The data were then fed into a computer to generate sections and plan maps, after making necessary corrections to the data.

Table II-1-6

Flow-chart of Model Analysis for Geophysical Survey



Two-dimensional models were prepared for promising anomalous zones to estimate the distribution patterns of anomaly sources, the characteristics of which were also analyzed by studying the variation in each frequency zone.

Table II-1--6 shows the general procedure of the model analysis.

### 1-2-2. Drilling Survey

As mentioned previously, the locations of drilling were determined in consideration of the results of the geochemical and geophysical surveys (IP and SIP), and of those of the past and current geological surveys. The drilling work was performed by a standard method using a diamond bit, and a number of core samples were collected.

The drilling cores were analyzed both petrologically and structurally to investigate their stratigraphical and structural characteristics. A study of mineral deposit was also conducted to investigate the nature and conditions of mineralization.

The necessary field work for the above mentioned studies and the selection of samples were undertaken at the CPRM's camp. Investigation of the drilling cores was made at intervals of 50 centimeters, and the data obtained in each 50-centimeter unit, including mineral compositions and metallic mineral contents, were recorded. The results of this study are compiled in a 1:200 scale columnar section for a unit core length of one-meter each (see Figure A-3). The mineral compositions and metallic mineral contents were judged under the naked eye on the field, and the quintuple semi-quantitative classification of each mineral was also made megascopically.

The drilling cores were photographed for a unit of two core boxes each, and close-up shots were taken for major mineralization parts. The selection of samples for tests and analyses was made at the same time, after the completion of the above mentioned investigation of the drilling cores.

Samples for electrical property tests were taken from the parts which were most likely to correspond to the electric survey, for each rock facies of different types. Samples for making thin sections were taken near the mineralization zones to make a close analysis of the mineralization. Test samples for polished sections were taken from the parts with representative characteristics of mineralization, and the samples for chemical assay were taken from the mineralization zones. The core samples were vertically divided into two parts, and the one half of each sample was used for various tests. As to the samples for electric property tests, pieces with

an approximate size of five centimeters were cut off from each sample, depending on the methods of measurement.

Ten thin sections, six polished sections, in addition to 60 samples for chemical assay and 26 samples for electric property tests were collected, and all of them except those for chemical assay were brought back to Japan for laboratory tests and analysis. The chemical assay was done in Brazil by a local company, Geosol.



## CHAPTER 2 SURVEY RESULTS

### 2-1 Results of Geophysical Survey

#### 2-1-1 Pseudosections

Pseudosections were prepared for all the survey lines, delineating an east-west profile of ten survey lines and a north-south profile of one line, as shown in Figures II-2-1 to II-2-12. No terrain corrections are given to the apparent resistivity pseudosections since the topography of the area is generally flat.

Interpretations for ten pseudosections are given below. In making these interpretations, apparent resistivity and PFE value are classified as follows:

	Apparent Resistivity	IP anomaly (PFE value)
High :	more than 1,000 $\Omega \cdot m$	more than 4 %
Medium :	500 - 1,000 $\Omega \cdot m$	3 - 4 %
Low :	less than 500 $\Omega \cdot m$	2 - 3 %

#### (1) Line 1330S (Figure II-2-8)

This survey line was set at the northmost part of the area.

Apparent resistivities are less than 500  $\Omega \cdot m$  at the both ends, and more than 1,000  $\Omega \cdot m$  in the central part. And the distribution pattern suggests the existence of a highly-resistive layer from the shallower part to the depth in the central part.

Low apparent resistivities are distributed between measuring points 70W and 30W, and at the east of measuring point 30E. The former shows the westward dip distribution from the ground surface, and the latter are distributed horizontally at the shallower part.

A strong IP anomalous zone is distributed in the high apparent resistivity zone.

#### (2) Line 1345S (Figure II-2-1)

The distribution of apparent resistivities in this line shows a similar pattern as that in the Line 1330S. In the western part of this line, a strong apparent resistivity contrast, suggesting the existence of the fault structure, is observed.

High apparent resistivities are predominantly distributed to the east of measuring point 50W.

Medium apparent resistivities are found in the shallower part to the east of measuring point

20E, which are the variation of low apparent resistivities at the east of measuring point 30E of the Line 1330S, and suggest the extension in the NS direction of the low to medium apparent resistivity zones.

Strong apparent resistivity contrast is found around measuring point 50W, suggesting the existence of the fault structure in general.

In this survey, phase differences of -20 to -25 milli-radian (mrad) correspond to the PFE values of 3.0 to 3.5 %, -25 to -30 mrad to 3.5 to 4.0 % (medium IP anomaly), and -30 mrad or less to 4.0 % or more (high IP anomaly), respectively.

Medium to high IP anomalous zones in Raw Phase, Three-Point Decoupled Phase and PFE pseudosections are distributed between measuring points 50W and 50E, and generally exhibit the same distribution pattern in each pseudosection. An IP anomaly of less than -30 mrad is observed in  $n=1$  to  $n=2$  (100 m to 150 m in depth) between measuring points 10W and 30E.

IP anomalies are concentrated in the high apparent resistivity zone.

### (3) Line 1360S (Figure II-2-9)

The distribution pattern of apparent resistivities in this line shows a similar pattern as that in the Line 1345S. And IP anomalies are concentrated in the central part.

High apparent resistivities are widely distributed between measuring points 60W and 90E. Medium apparent resistivities are sporadically distributed in the shallower part, in addition to  $n=1$  to  $n=4$  (100 m to 250 m in depth) between measuring points 20E and 90E. And low apparent resistivities are found only to the west of measuring point 70W.

IP anomalies of more than 3.0 % are distributed between measuring points 40W and 30E, suggesting the existence of the evenly impregnated anomalous source (disseminated zone). High IP anomaly of more than 4.0 % is found in the shallower part between measuring points 20W and 10W.

### (4) Line 1375S (Figure II-2-2)

A strong apparent resistivity contrast with eastward dip, possibly reflecting a fault structure, is found between measuring points 10E and 60E. And medium apparent resistivities, thought to reflect a low resistivity layer at the ground surface, is distributed in the shallower part to the west of measuring point 10W.

High apparent resistivities are distributed in three parts divided by medium apparent resistivities, between measuring points 60W and 30W, between 10W and 50E, and to the east of 60E.

While, medium apparent resistivities are locally found in the shallower part between measuring points 30W and 20W and between 10E and 50E. The former shows eastward dip, and the latter may be due to the weathering and/or groundwater.

The following three IP anomalies, zones, which are caused by IP anomalous sources in the shallower part, are distributed between measuring points 30W and 80E;

- 1) IP anomaly centered around  $n=1$  (100 m in depth) between measuring points 30W and 20W.
- 2) IP anomaly distributed at a shallower depth than  $n=1$  (100 m in depth) between measuring points 10E and 20E, with a slight dip toward the west.
- 3) IP anomaly distributed at a depth shallower than  $n=2$  (150 m in depth) to the east of measuring point 80E.

**(5) Line 1390S (Figure II-2-10)**

Apparent resistivities show a distribution pattern slightly different from those observed in the northern lines, and also IP anomalies are weaker than those in the northern lines.

High apparent resistivities are found from the ground surface to the depth between measuring points 10W and 10E, and between 60E and 70E. Between measuring points 50W and 40E, however, they are widely distributed at the depth of more than  $n=3$  (200 m in depth). On the other hand, low apparent resistivities are found to the west of measuring point 80W, between 30W and 20W, and at the shallower part between 10E and 50E. The existence of a fault structure is inferred between measuring points 30W and 20W.

Notable IP anomalies are found in the high apparent resistivity zone of the east of a strong resistivity contrast observed between measuring points 30W and 10E. These IP anomalies dipping slightly toward the east seem to be due to the shallower IP anomalous sources.

**(6) Line 1405S (Figure II-2-3)**

An apparent resistivity pseudosection shows a complex distribution pattern which is considered to reflect a complicated resistivity structure with notable clustering into blocks. This tendency of the pattern is also observed in the Line 1390S.

High apparent resistivities are distributed in the depth between measuring points 50W and 20W, between 10E and 50E and to the east of 60E. While low apparent resistivities, which suggest the existence of fault structures, are distributed between measuring 0 and 10E and in province of 70E, at the whole depth with a slight dip toward the west, in such a manner as to divide the high apparent resistivity zone distributed broadly in depth. They are also found to the west of

measuring point 10W, and are distributed in the shallower part up to measuring point 60W, extending to the depth in the west of measuring point 70W.

Two IP anomalies are found between measuring points 50W and 0, and between 30E and 60E. The former IP anomaly shows a distribution pattern to be formed by three anomalous sources. One of those is distributed in the depth with a westward dip, between measuring points 50W and 60W. The other two are distributed from the shallower part to the middle depth with eastward dip, between measuring points 30W and 20W, and between 20W and 10W, respectively. The IP anomalous source of the latter IP anomaly is distributed at the depth of 200 m to 250 m between 30E and 50E.

(7) Line 1420S (Figure II-2-4, Figure II-2-11)

On the whole, apparent resistivities on this line are distributed in two zones, with the boundary around measuring point 10E. And the distribution of IP anomalies in this line covers an area wider than that in Line 1405S.

High apparent resistivities are found between measuring points 30W and 20W, and between 10E and 80E. The former are distributed in depth in such a manner as being overlain by low apparent resistivities stretching to the west of measuring point 10E, and the latter are distributed locally within the medium apparent resistivity zone.

IP anomalies are concentrated between measuring points 20W and 60E. IP anomalous zone of PFE of more than 4.0 % is found in the medium-to-high apparent resistivity zone between measuring points 10E and 50E. This distribution pattern suggests that this zone may be due to the dissemination zone distributed from the surface, the most concentrated part of which may be located at the depth between 150 m and 200 m below measuring point 30E.

(8) Line 1430S (Figure II-2-5)

Low-to-medium apparent resistivities are widely distributed in this line, but no high apparent resistivity was found. IP anomalies are concentrated in the central part, showing a similar distribution pattern as that in the Line 1420S.

Low-to-medium apparent resistivities are widely distributed in this line, but no high apparent resistivity was found. IP anomalies are concentrated in the central part, showing a similar distribution pattern as that in the Line 1420S.

reflect the fault structure and the accompanying fracture zone. Medium apparent resistivities are distributed in blocks at the depth of more than 150 m between measuring points 40W and 10W,

and from the ground surface between measuring points 10E and 60E.

IP anomalies with phase-differences of less than -30 mrad are found between measuring points 20W and 10W and between 0 and 40E, and they are distributed at the portion of notable apparent resistivity variations. The former IP anomaly shows a westward dip at the depth of more than 150 m, and the latter is distributed with eastward dip from the ground surface.

IP anomalies in this line show the most strong IP effects among those in the lines discussed above. This fact suggests that much sulfides may exist in the IP anomalous zone of this line.

**(9) Line 1440S (Figure II-2-12)**

Distribution pattern of apparent resistivities suggests that the geological structure of the survey area is more complicated in the southern part than in other parts. And IP anomalies become also weaker in the southern part.

Low apparent resistivities are found on the whole pseudosection. While medium apparent resistivities are distributed on a small scale below measuring point 50W, between 40W and 10E, between 10E and 50E, and below 70E.

An IP anomaly of PFE of 3 % to 4 % is distributed with a westward dip between measuring points 10W and 60E, suggesting to be due to several small-scale IP anomalous sources dipping toward west.

**(10) Line 1450S (Figure II-2-6)**

The distribution pattern of apparent resistivities in this line is similar to that in Line 1440S. However, IP anomalous zones are of small-scale.

Low apparent resistivity zones are dipping toward the east and toward the west at the westmost and eastmost ends of the pseudosection, respectively. But those are distributed horizontally in the central part of the pseudosection. Medium apparent resistivities are distributed at the depth of more than 200 m between measuring points 30W and 30E and between 30E and 40E.

Two IP anomalies are distributed with westward dip between measuring points 40W and 20W and between 00 and 20E. The former IP anomaly shows a westward dip in the Raw-Phase and 3-pt Decoupled-Phase pseudosections, but it is diminished in the PFE pseudosection. This is presumably due to the spectral changes caused by the local geological differences.

(11) Line-20E (Figure II-2-7)

High apparent resistivities of more than  $100 \Omega \cdot m$  are distributed to the north of measuring point 1410S. This distribution pattern suggests that the high resistivity layer exists from the shallow part to the depth at the northern part of measuring point 1370S, and it dips southward at the southern part of 1370S.

Low apparent resistivities of less than  $500 \Omega \cdot m$  are distributed to the south of measuring point 1450S. This distribution pattern means the measuring point 1450S may be due either to the boundary of layers or fault structures.

Medium apparent resistivities between  $500 \Omega \cdot m$  and  $1000 \Omega \cdot m$  are widely distributed in the central part of this line.

High IP anomalies of more than 4.0% are found inside the high apparent resistivity zone at the north of measuring point 1370S and inside also the medium apparent resistivity zone between measuring points 1410S and 1440S.

Distribution pattern at the north of measuring point 1370S is not clear, because that is detected at the northern-end of this line. Due to the reason that the IP anomalies of other east-west lines are continuous, this IP anomalous zone may be also the continuation of the IP anomalous zone centered measuring point 20E in Line-1345S.

The center of high IP anomaly between 1410S and 1440S indicate PFE value of more than 4.5% between measuring point of 1420S and 1430S. This distribution pattern suggests the existence of IP anomalous source from the shallower part to the depth of 150m.

### 2-1-2 Plan Maps

The plan maps were prepared based on apparent resistivity maps (Figures II-2-13 to II-2-15) and PFE maps (Figures II-2-16 to II-2-18). Depth levels of the plan maps are  $n=1$ ,  $n=3$  and  $n=5$ , each of which is considered to reflect information from the depths of 100 m, 200 m and 300 m below the ground surface, respectively.

The same classifications for apparent resistivities and IP anomalies as those in the pseudo-section (2-1-1) are adopted.



Line-1345S

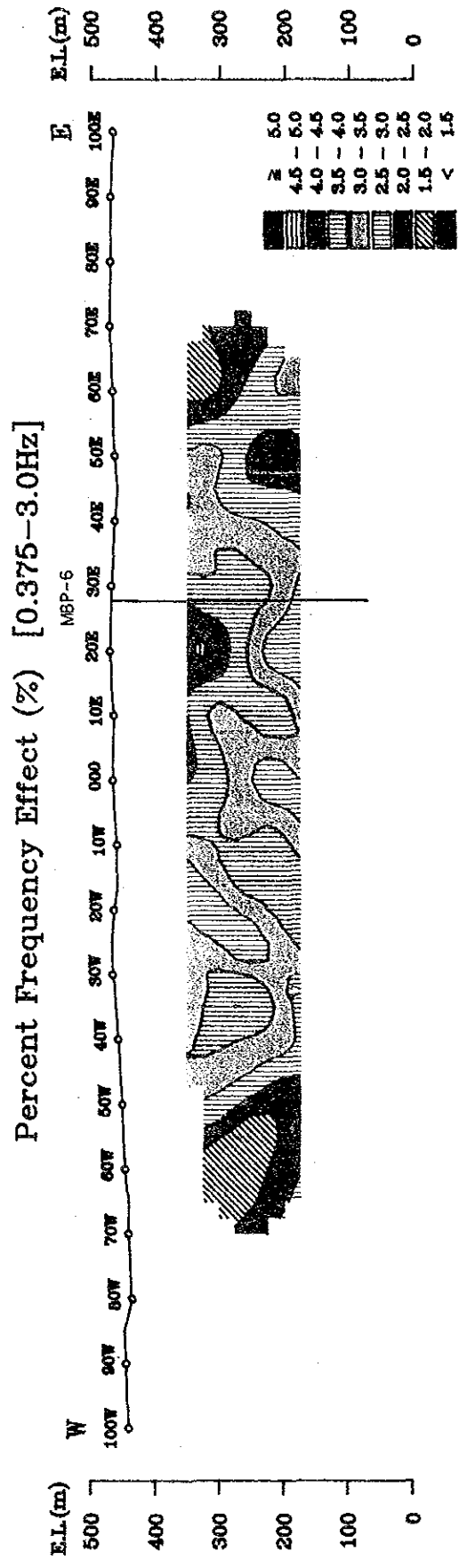
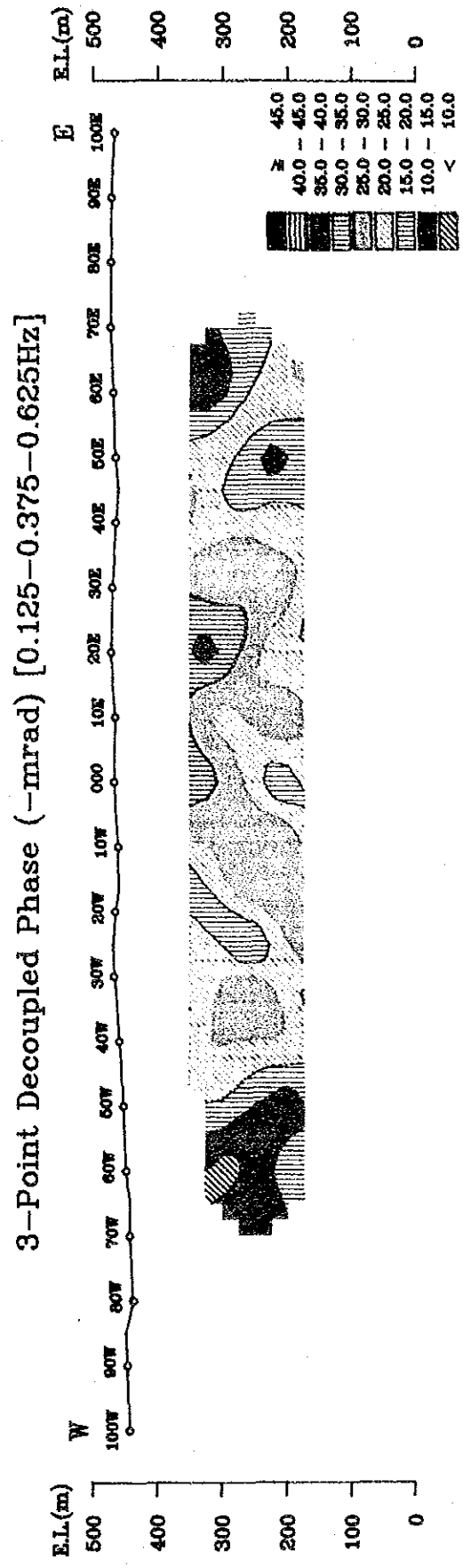
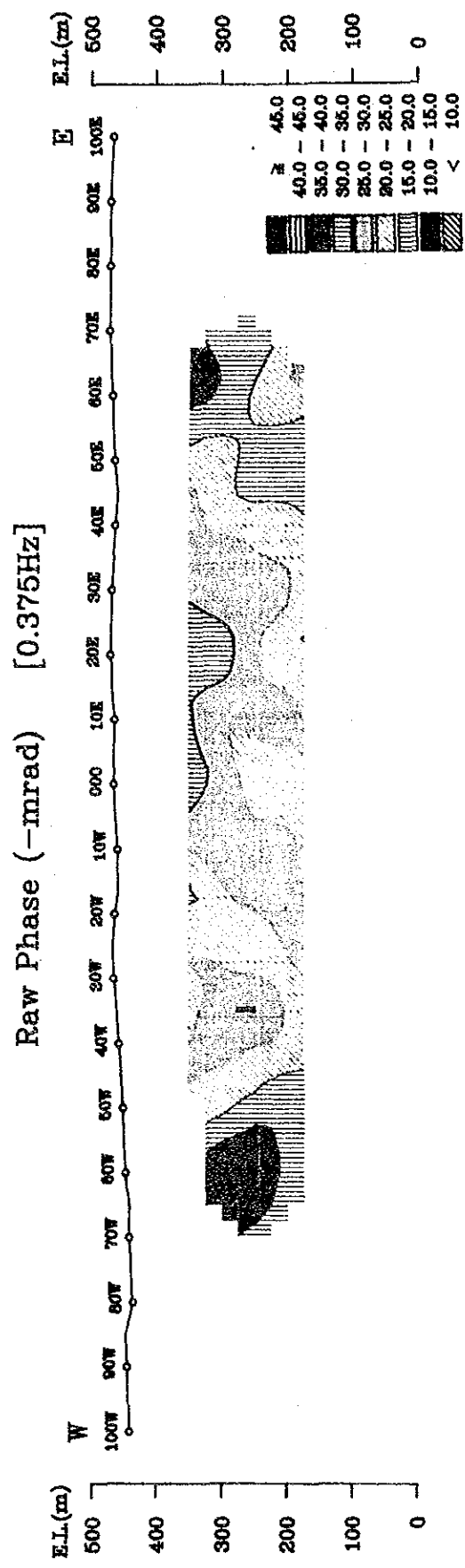
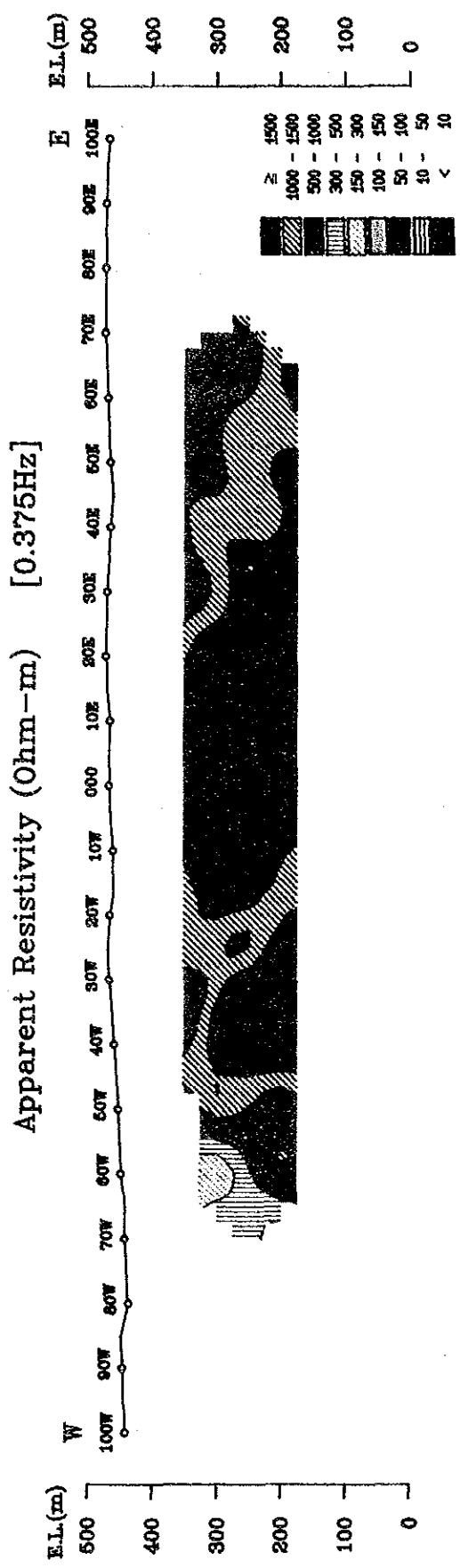


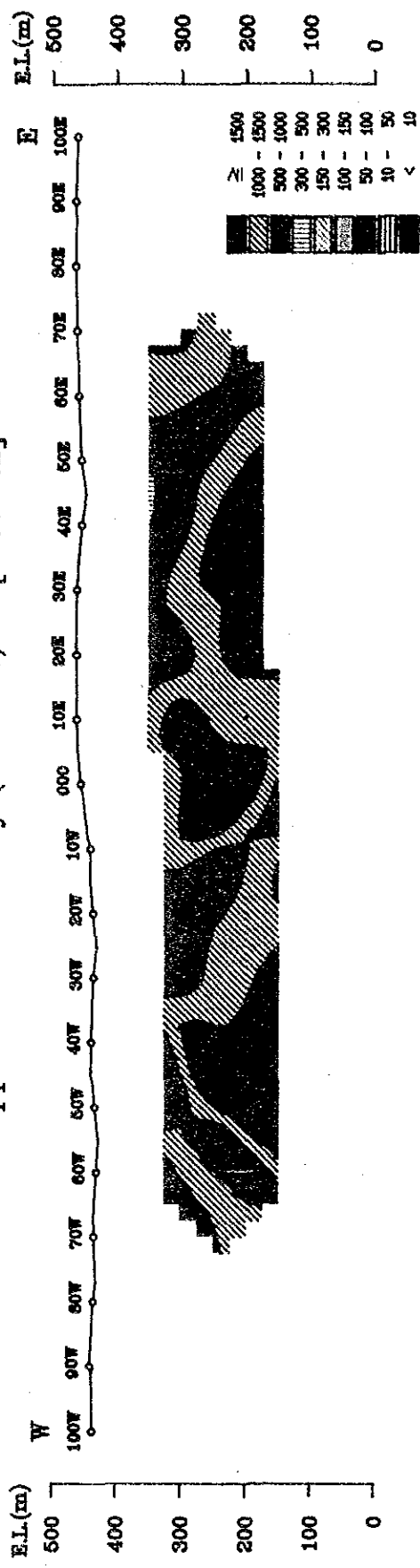
Fig. II-2-1 SIP Pseudo-Section (Line-1345S)



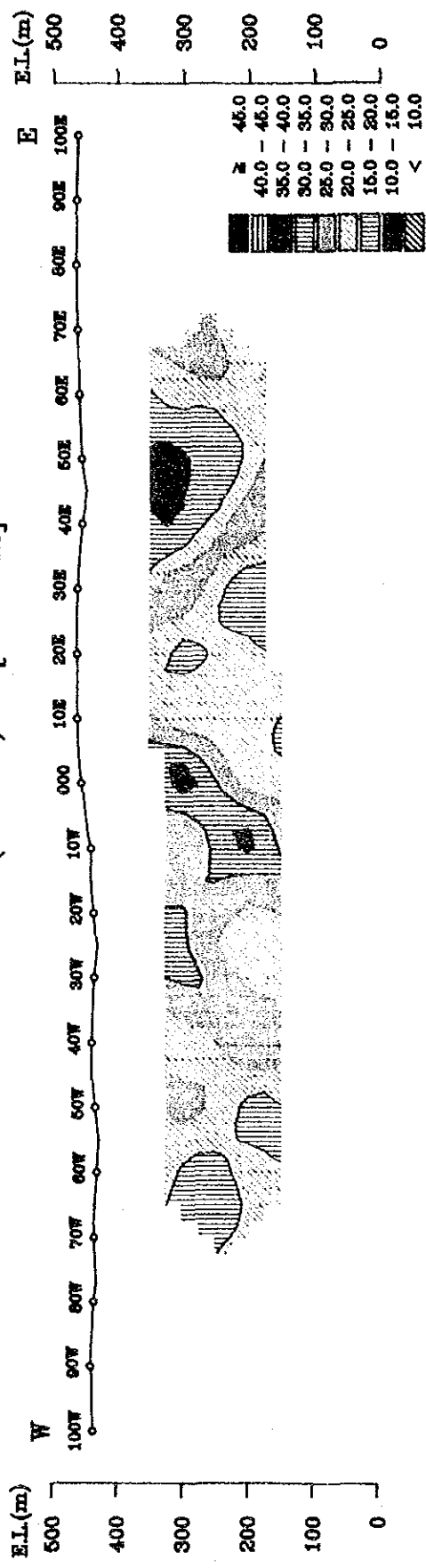


# Line-1375S

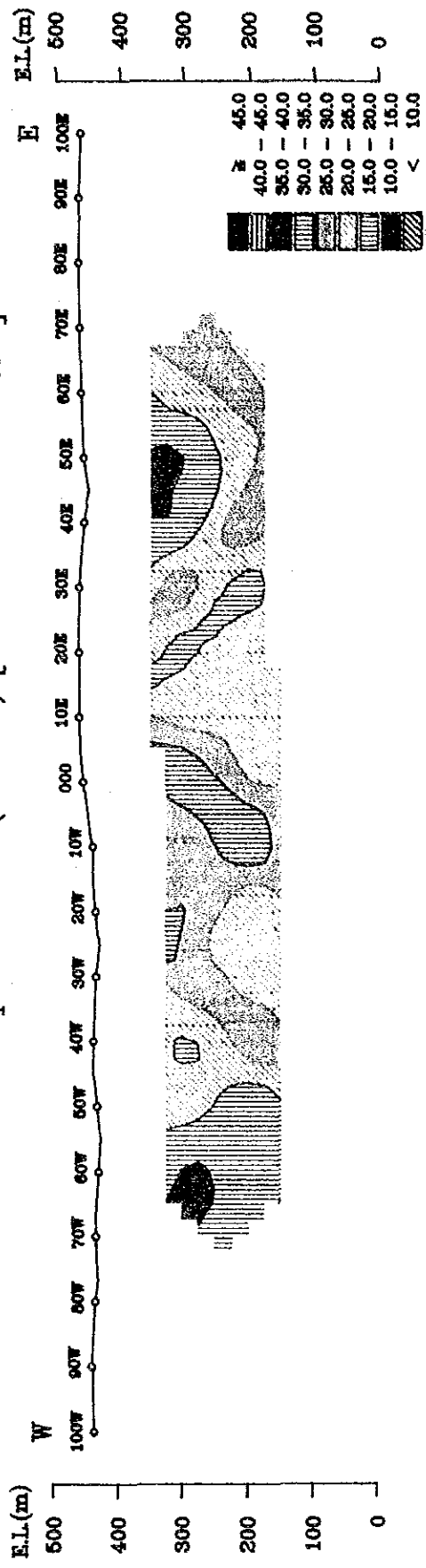
Apparent Resistivity (Ohm-m) [0.375Hz]



Raw Phase (-mrad) [0.375Hz]



3-Point Decoupled Phase (-mrad) [0.125-0.375-0.625Hz]



Percent Frequency Effect (%) [0.375-3.0Hz]

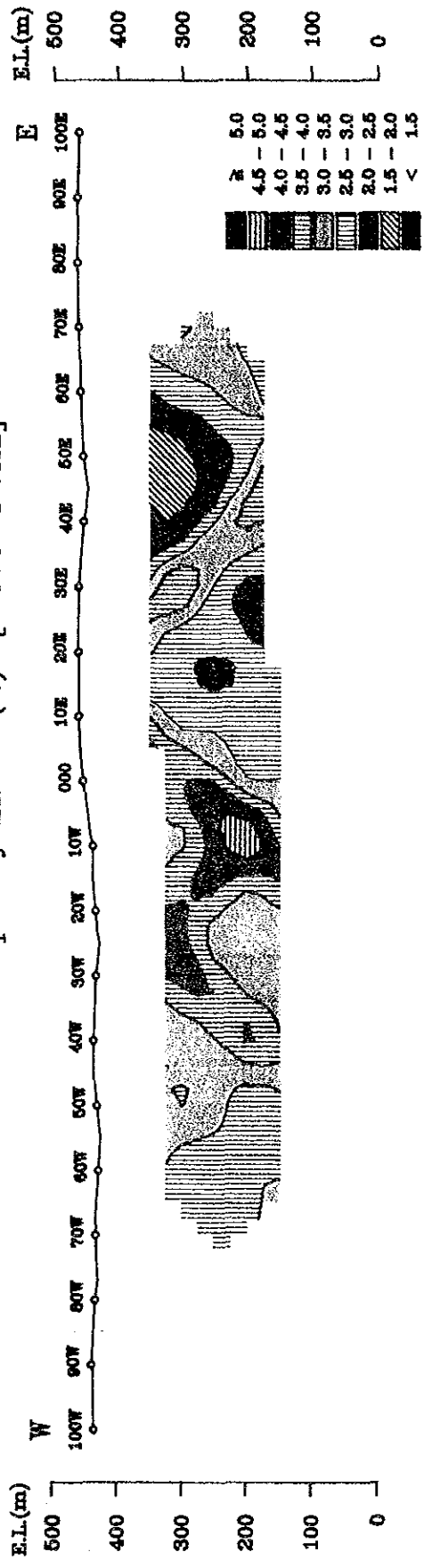


Fig. II-2-2 SIP Pseudo-Section (Line-1375S)



Line-1405S

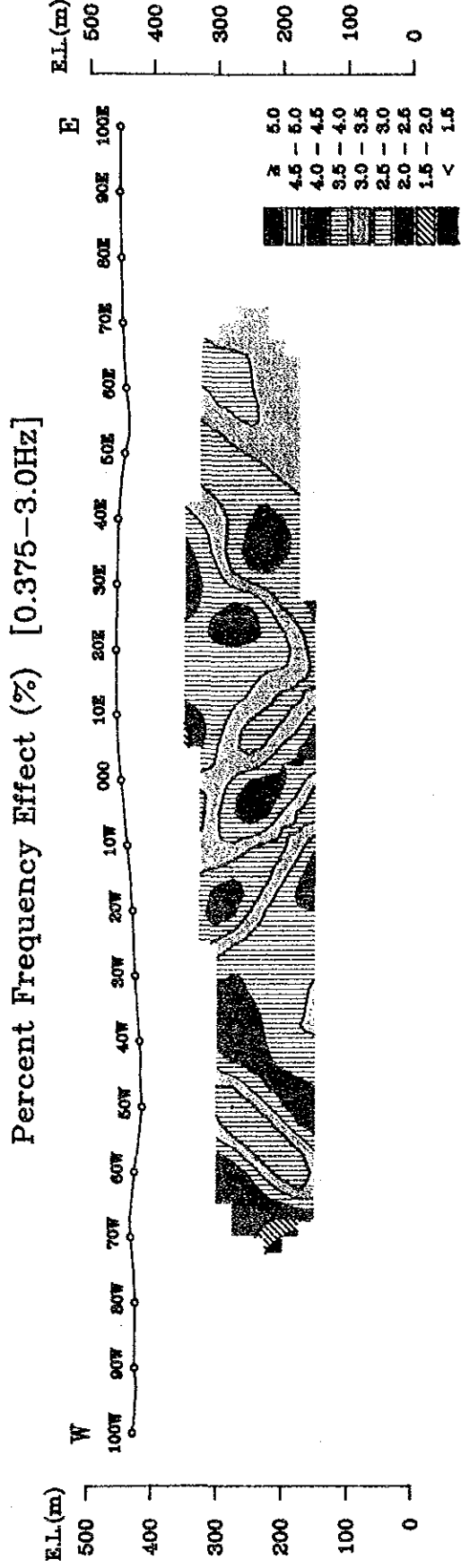
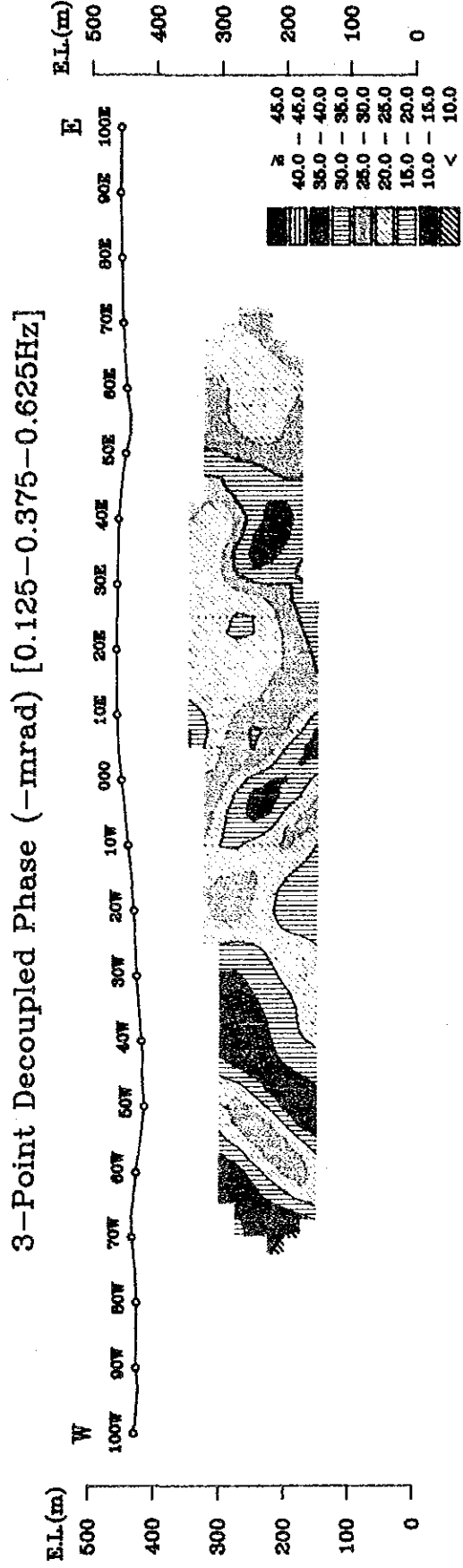
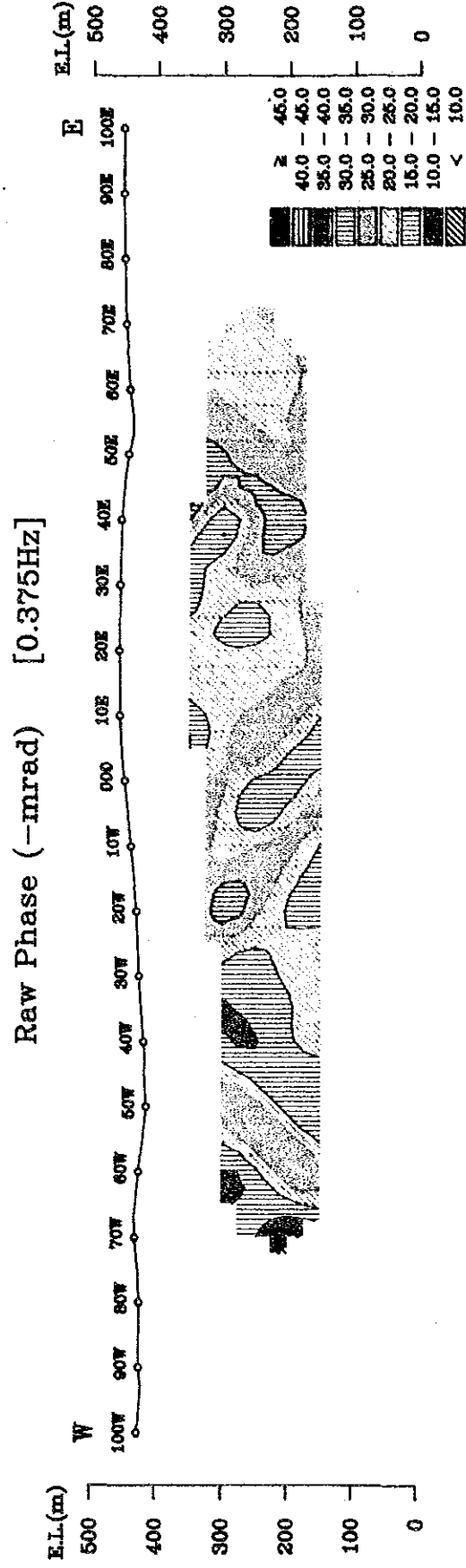
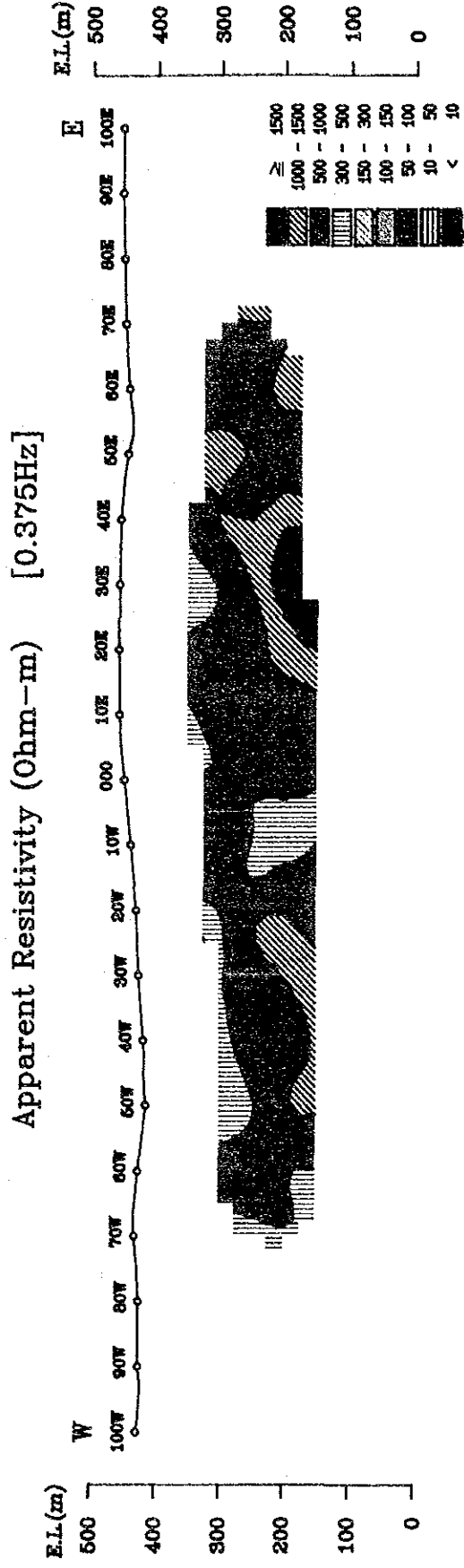
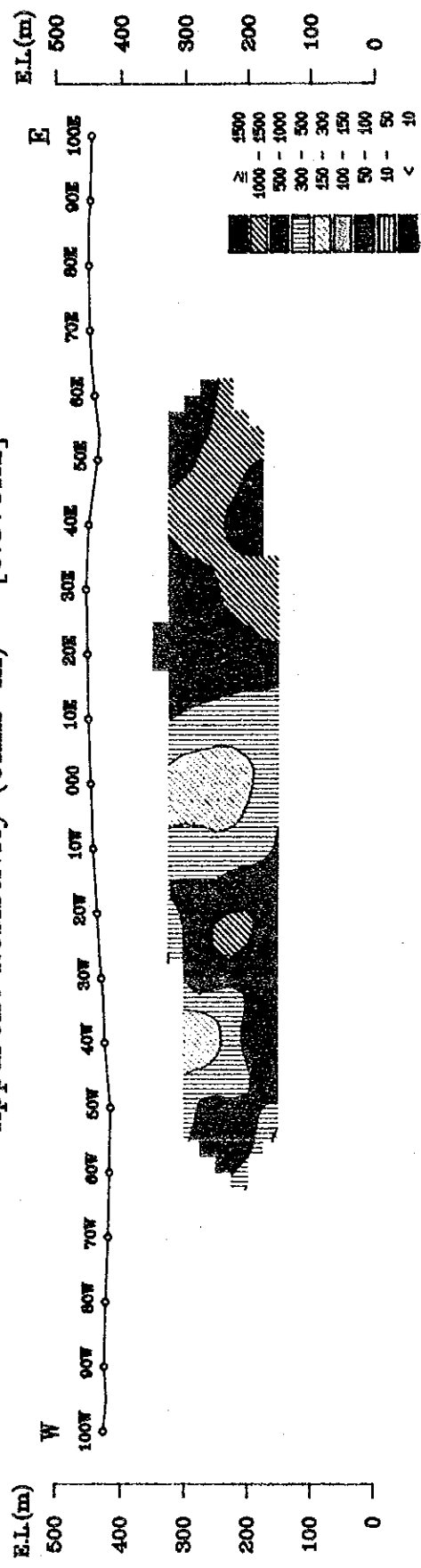


Fig. II-2-3 SIP Pseudo-Section (Line-1405S)

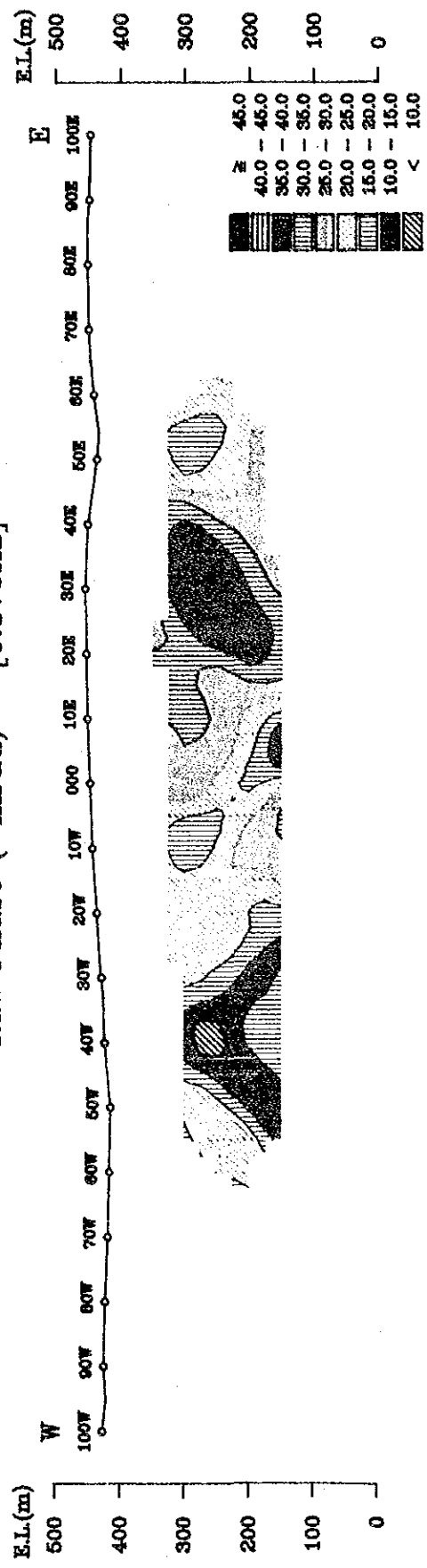


# Line-1420S

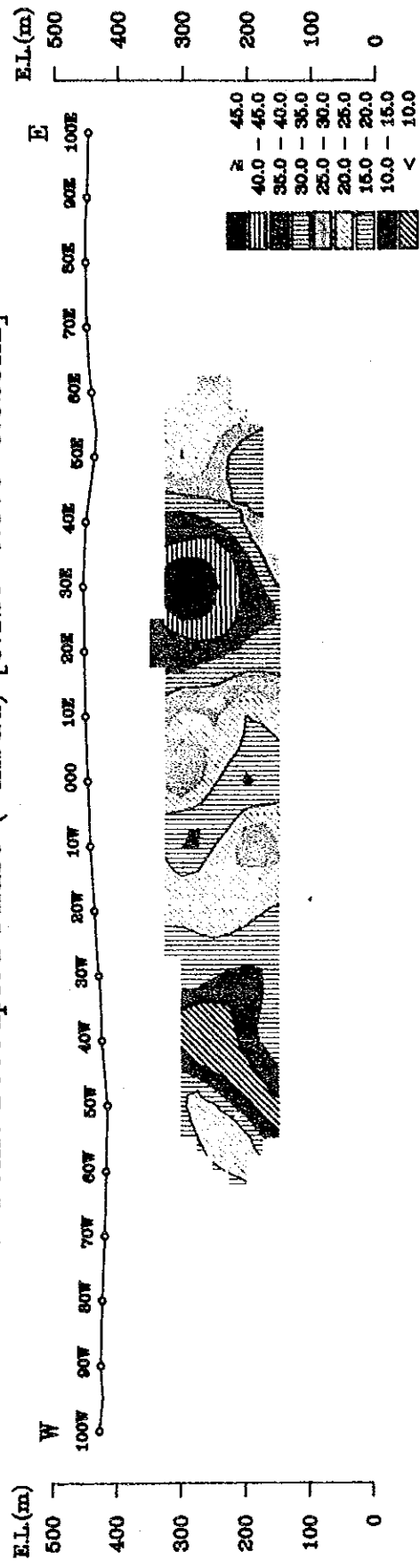
Apparent Resistivity (Ohm-m) [0.375Hz]



Raw Phase (-mrad) [0.375Hz]



3-Point Decoupled Phase (-mrad) [0.125-0.375-0.625Hz]



Percent Frequency Effect (%) [0.375-3.0Hz]

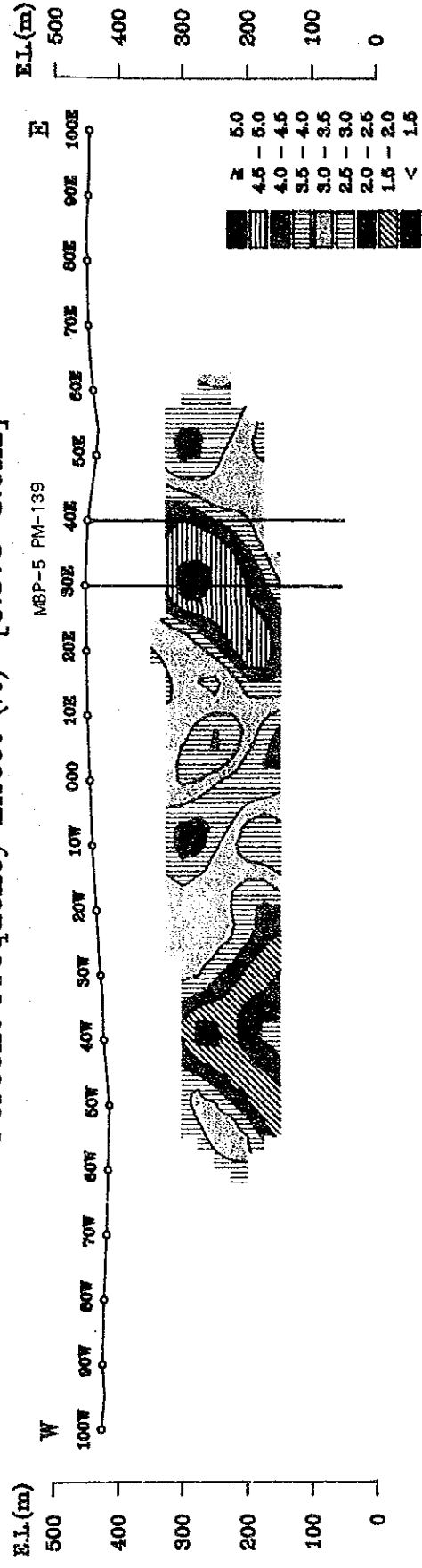


Fig. II-2-4

SIP Pseudo-Section (Line-1420S)



Line-1430S

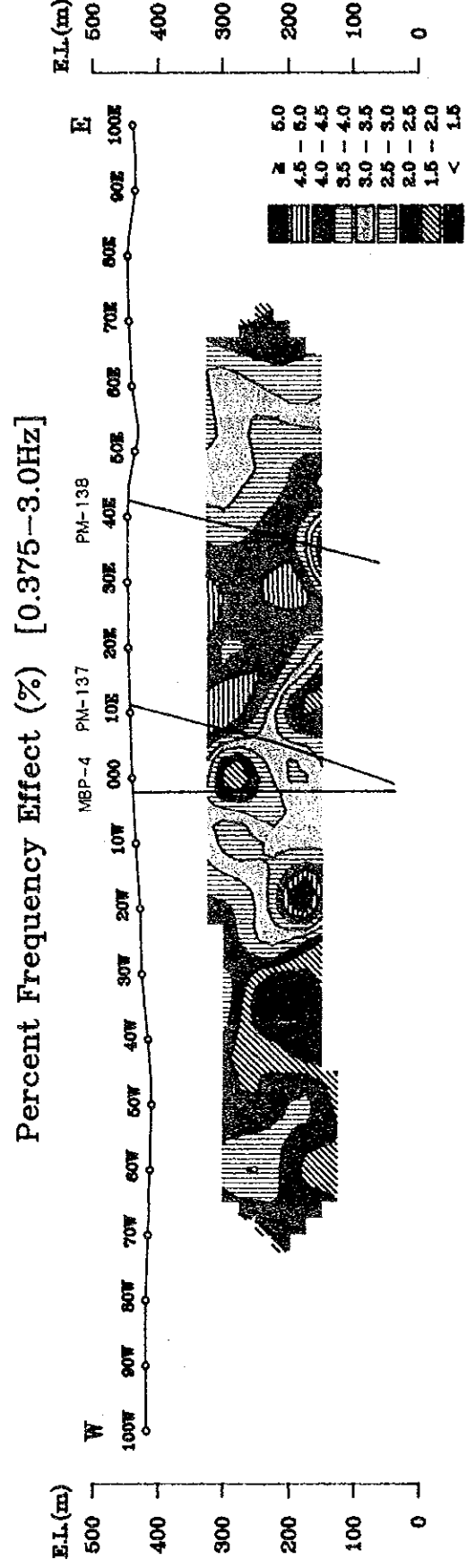
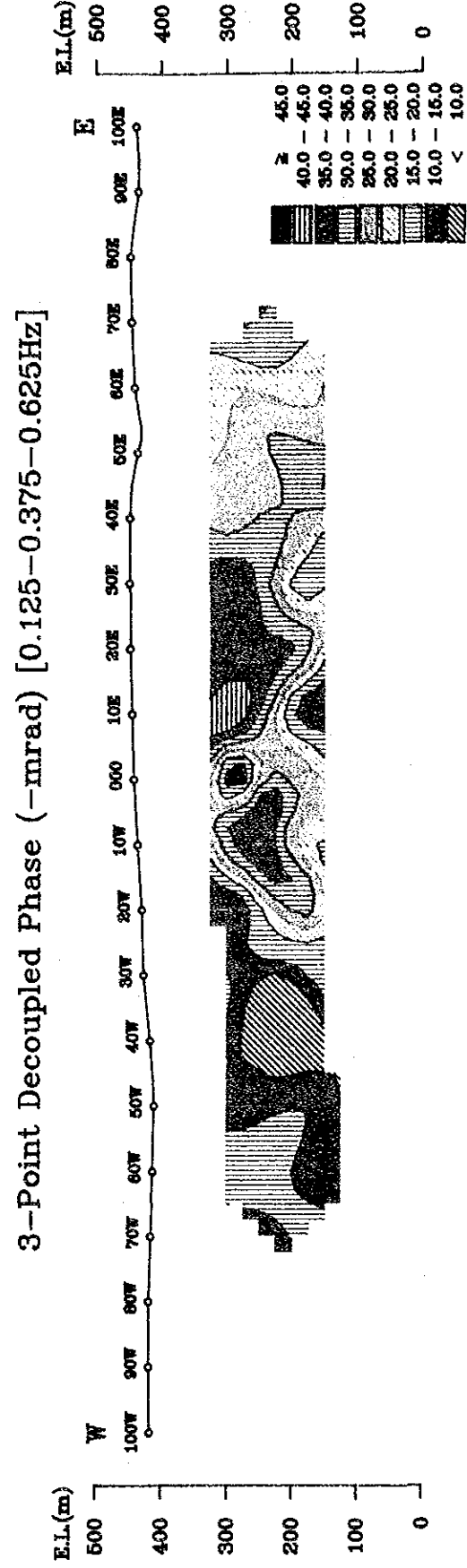
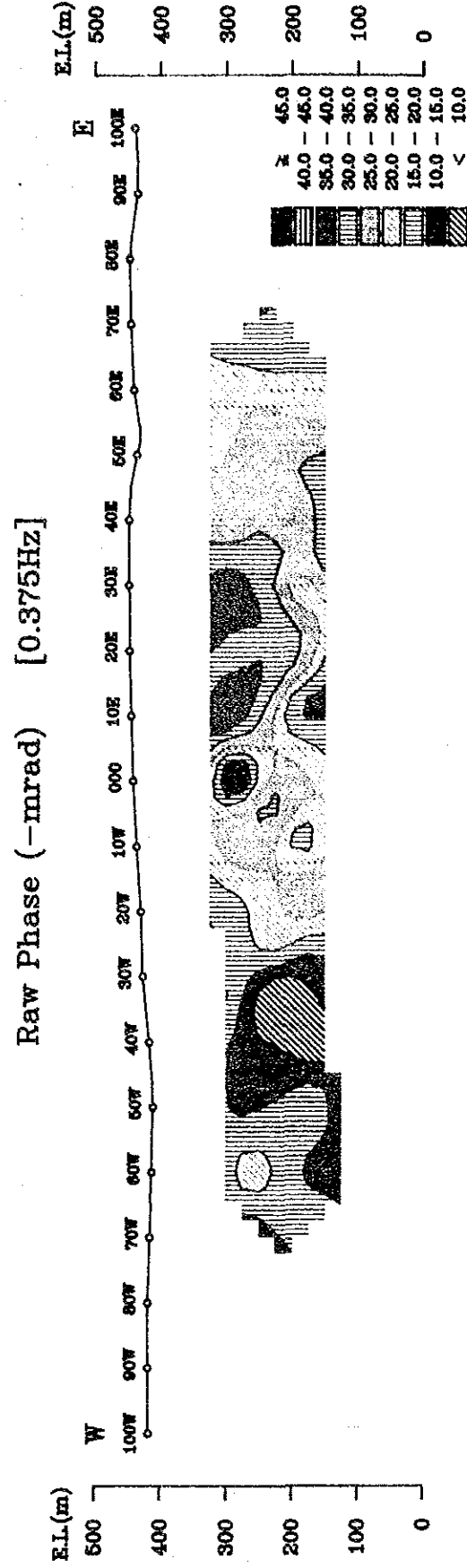
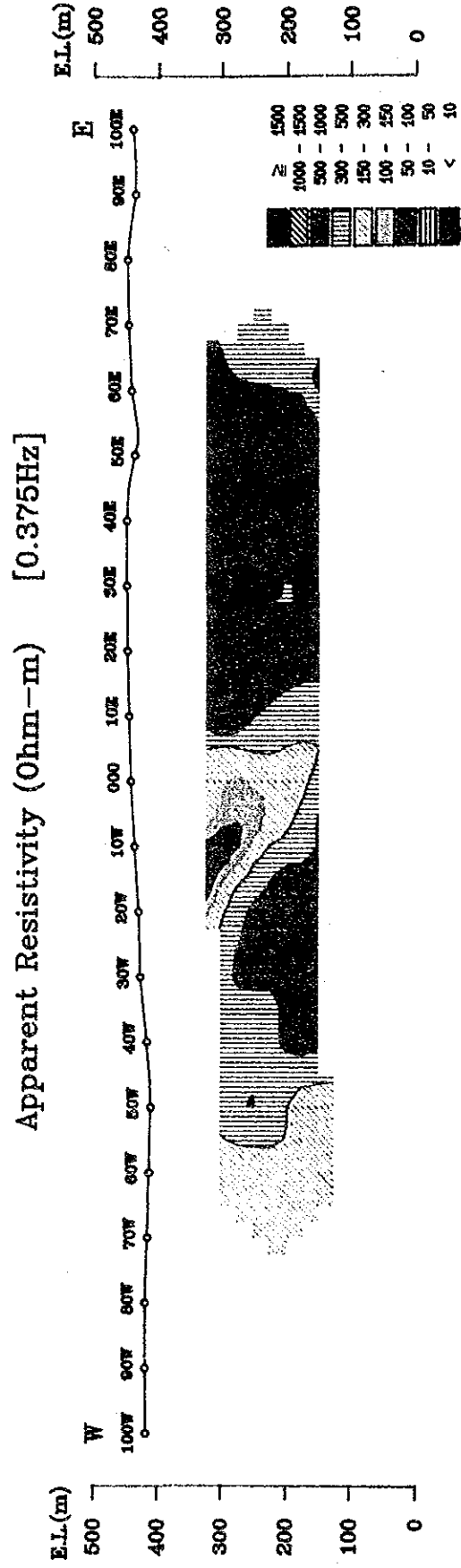


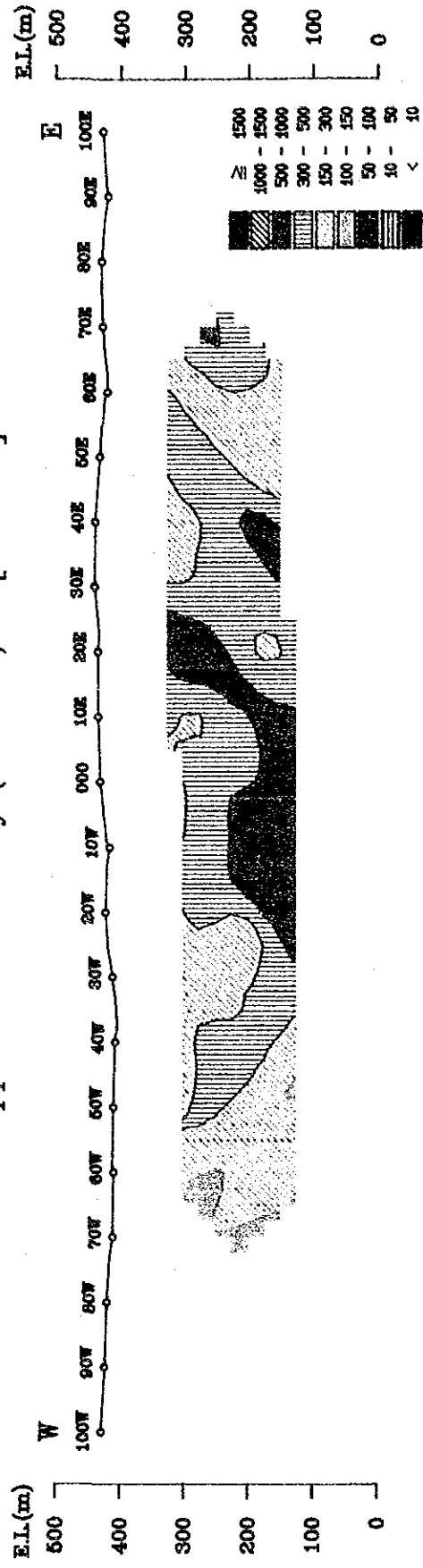
Fig. II-2-5 SIP Pseudo-Section (Line-1430S)



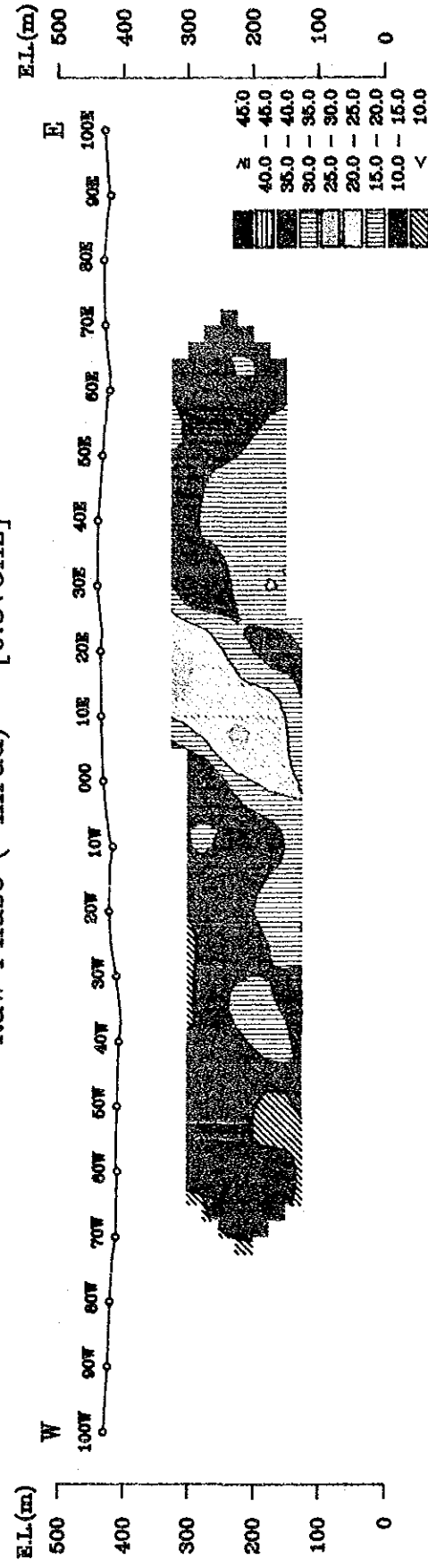


Line-1450S

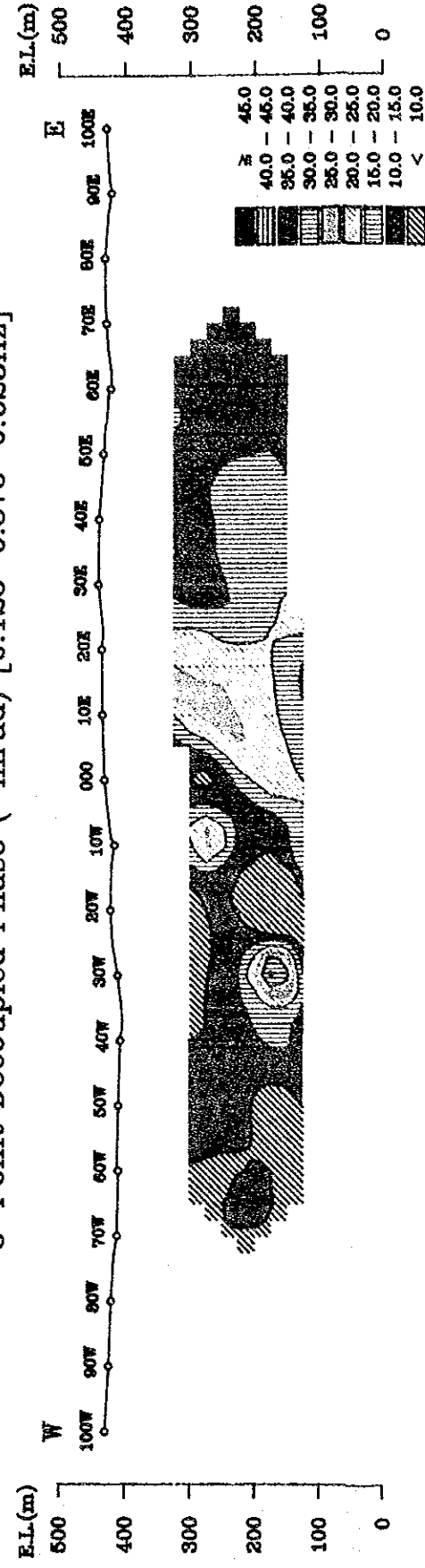
Apparent Resistivity (Ohm-m) [0.375Hz]



Raw Phase (-mrad) [0.375Hz]



3-Point Decoupled Phase (-mrad) [0.125-0.375-0.625Hz]



Percent Frequency Effect (%) [0.375-3.0Hz]

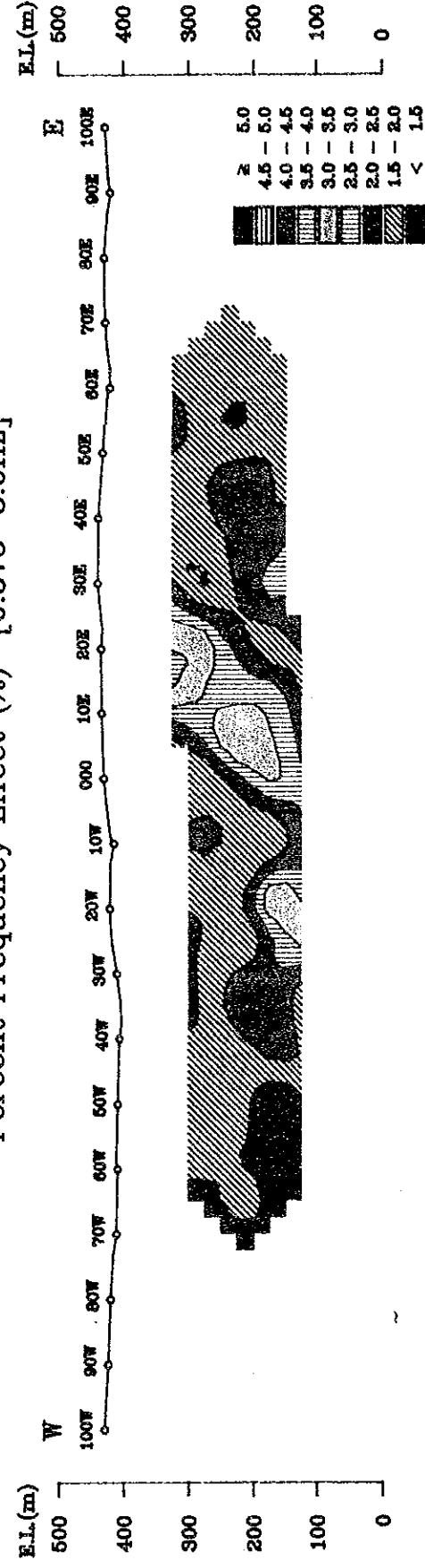


Fig. II-2-6 SIP Pseudo-Section (Line-1450S)



Line-20E

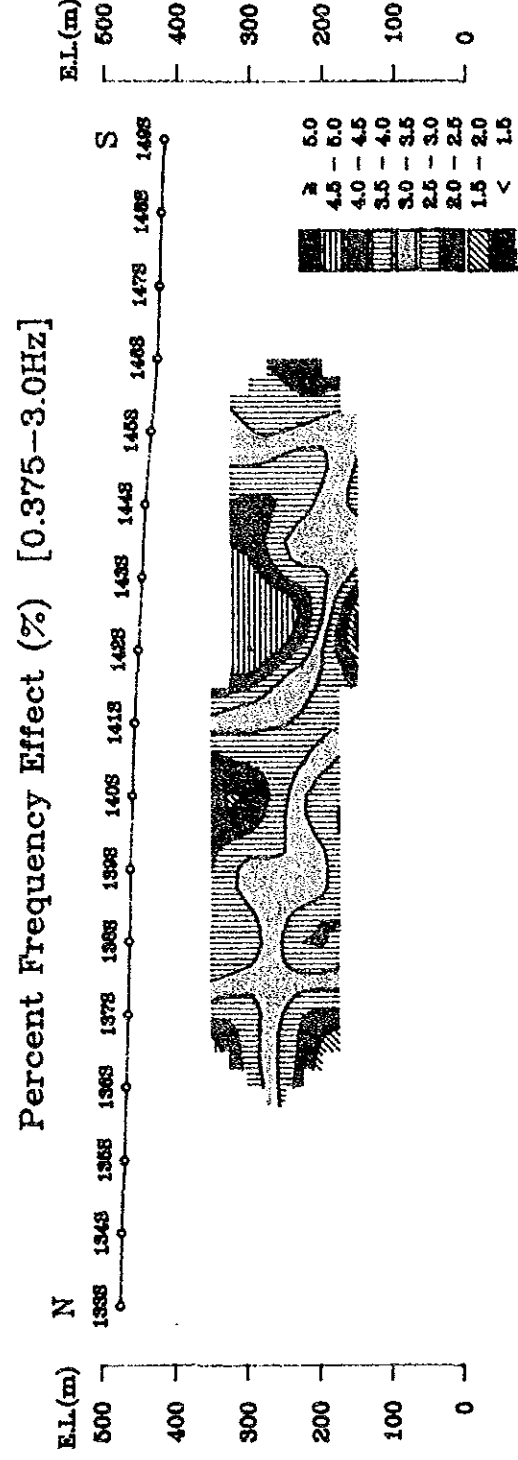
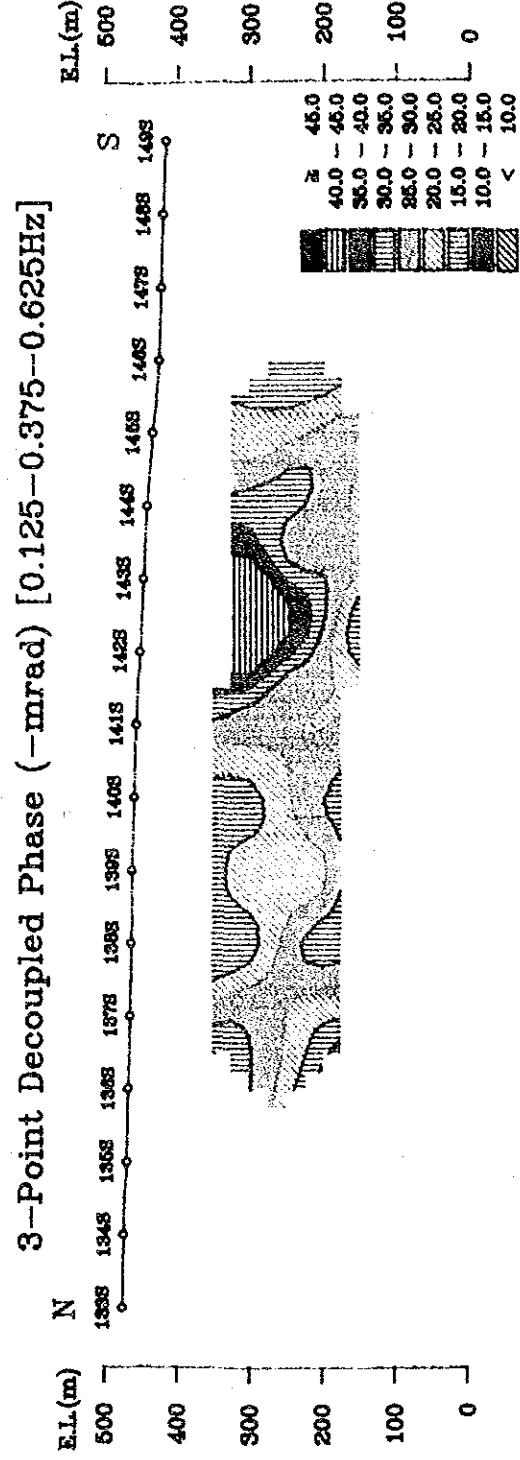
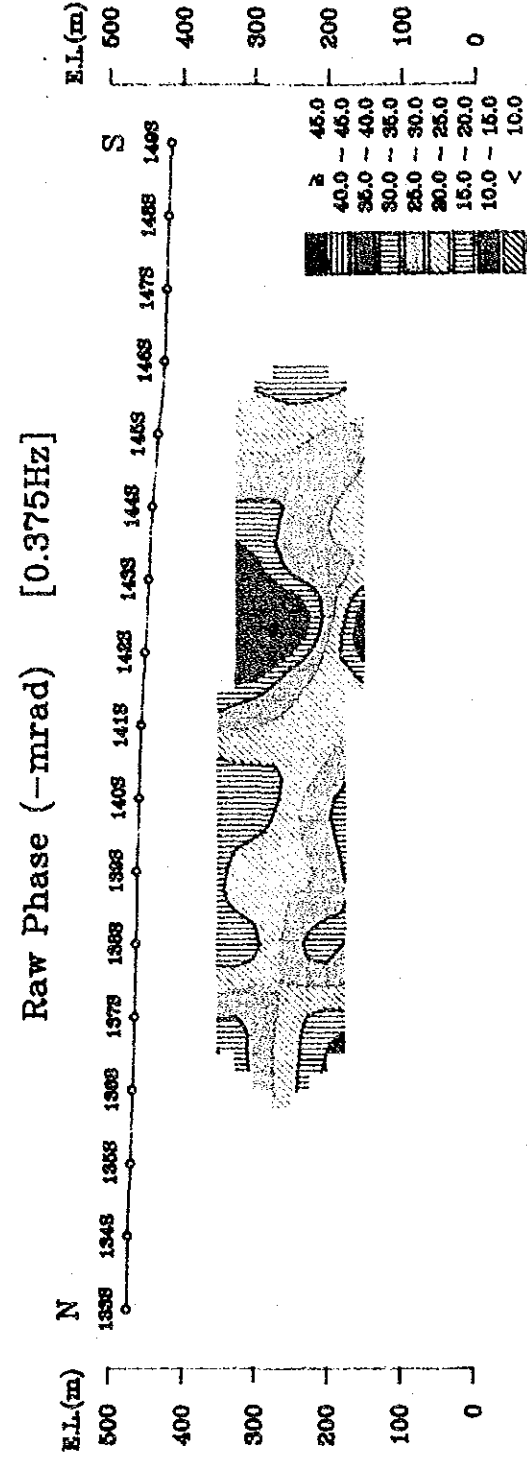
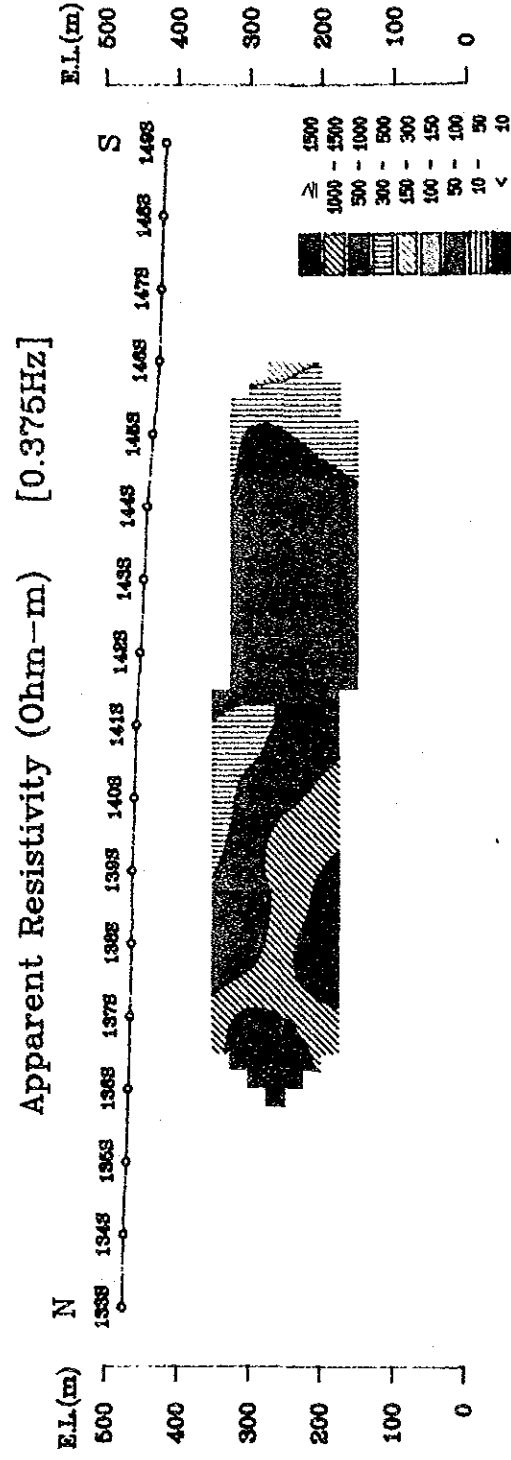
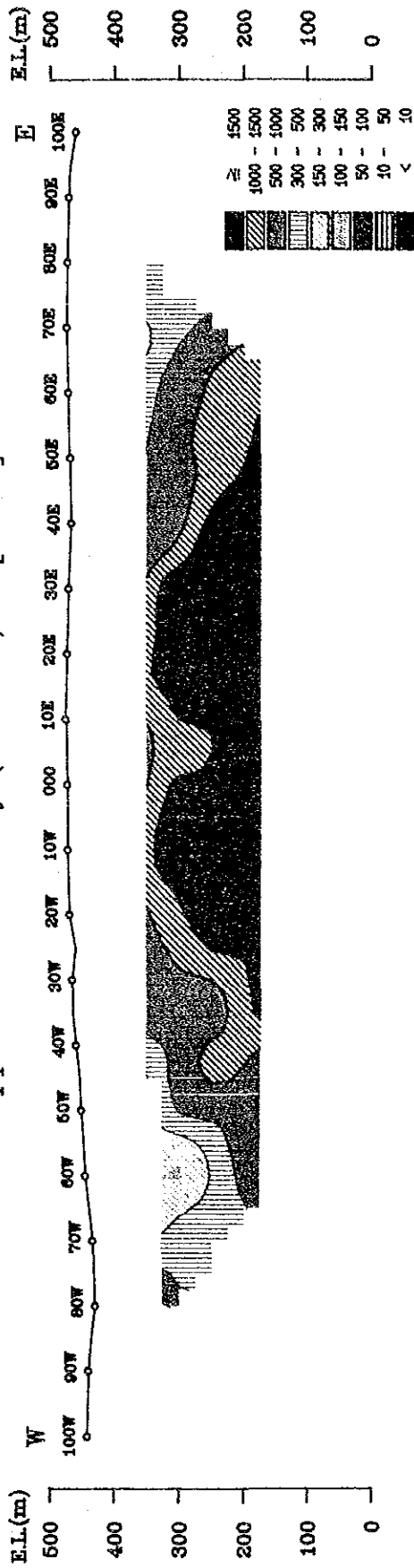


Fig. II-2-7 SIP Pseudo-Section (Line-20E)



# Line-1330S

## Apparent Resistivity (Ohm-m) [0.3Hz]



## Percent Frequency Effect (%) [0.3-3.0Hz]

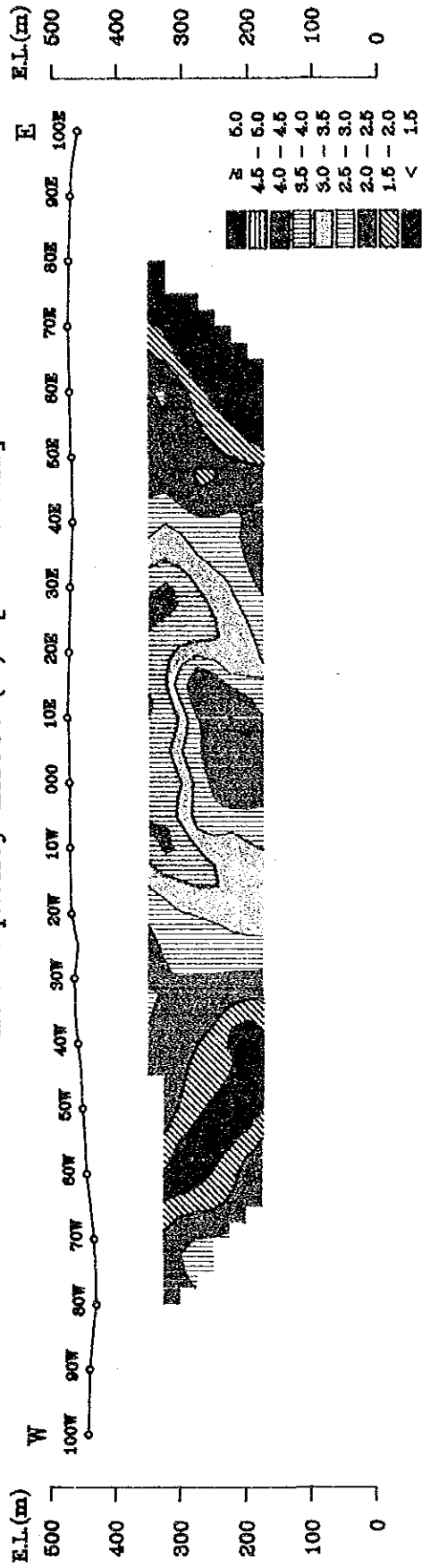
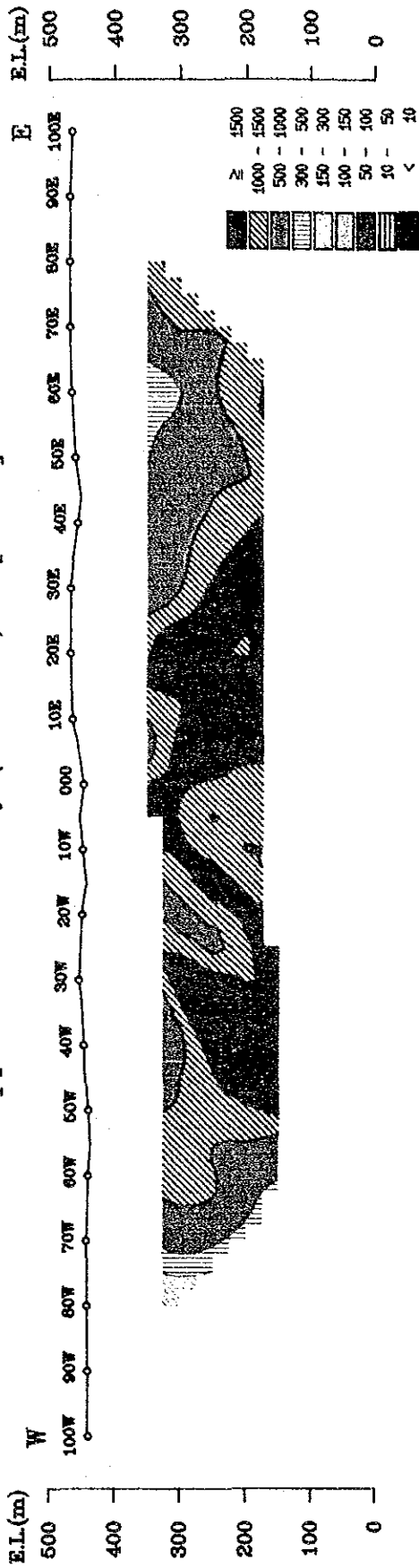


Fig. II-2-8 IP Pseudo-Section (Line-1330S)



# Line-1360S

Apparent Resistivity (Ohm-m) [0.3Hz]



Percent Frequency Effect (%) [0.3-3.0Hz]

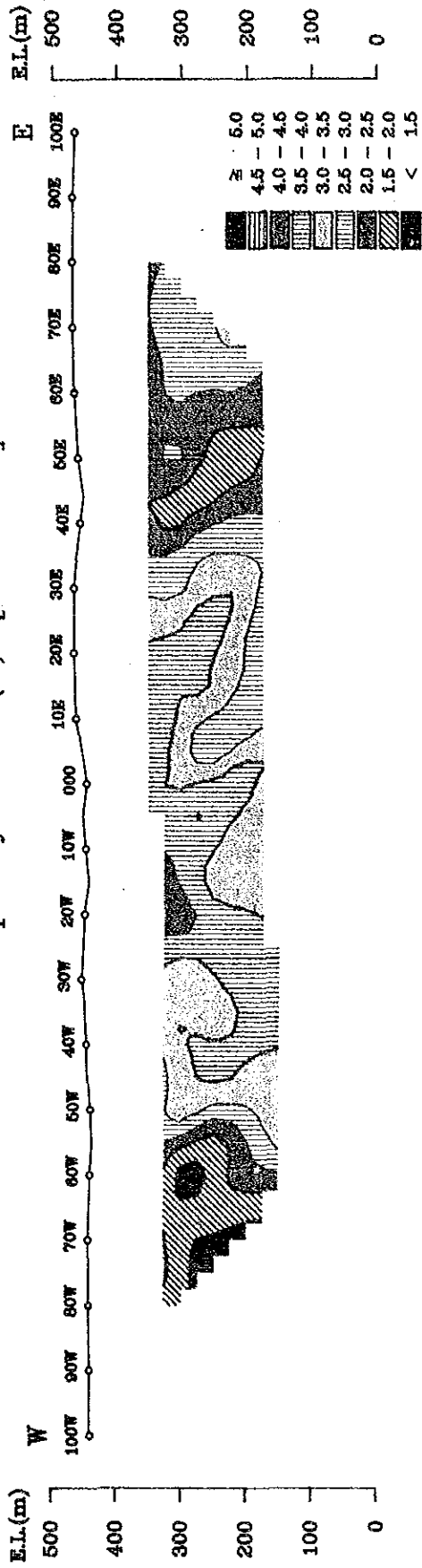


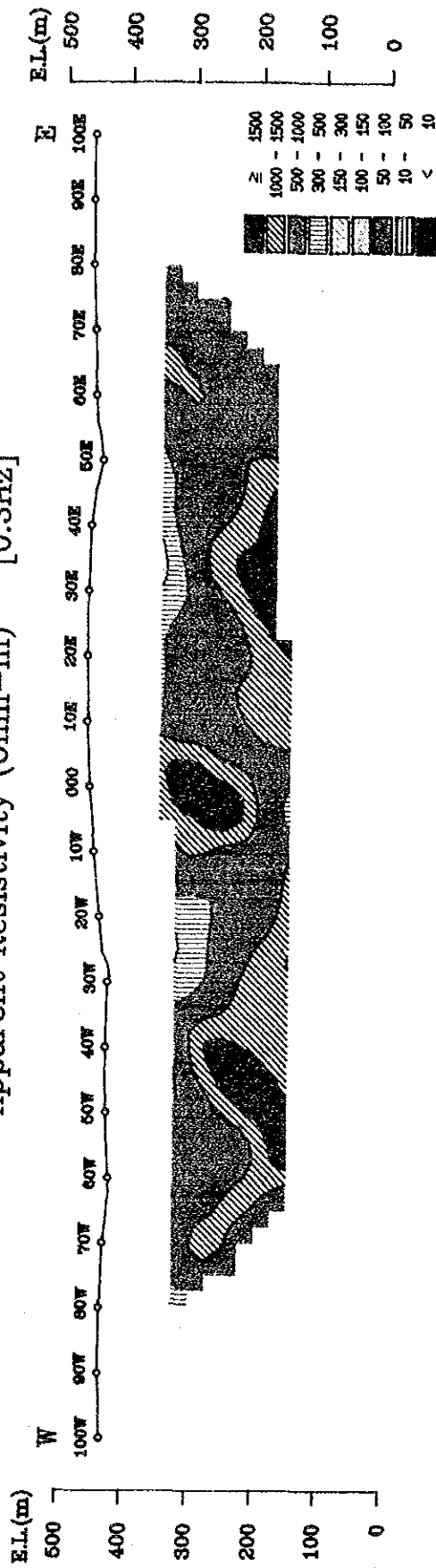
Fig. II-2-9 IP Pseudo-Section (Line-1360S)





# Line-1390S

Apparent Resistivity (Ohm-m) [0.3Hz]



Percent Frequency Effect (%) [0.3-3.0Hz]

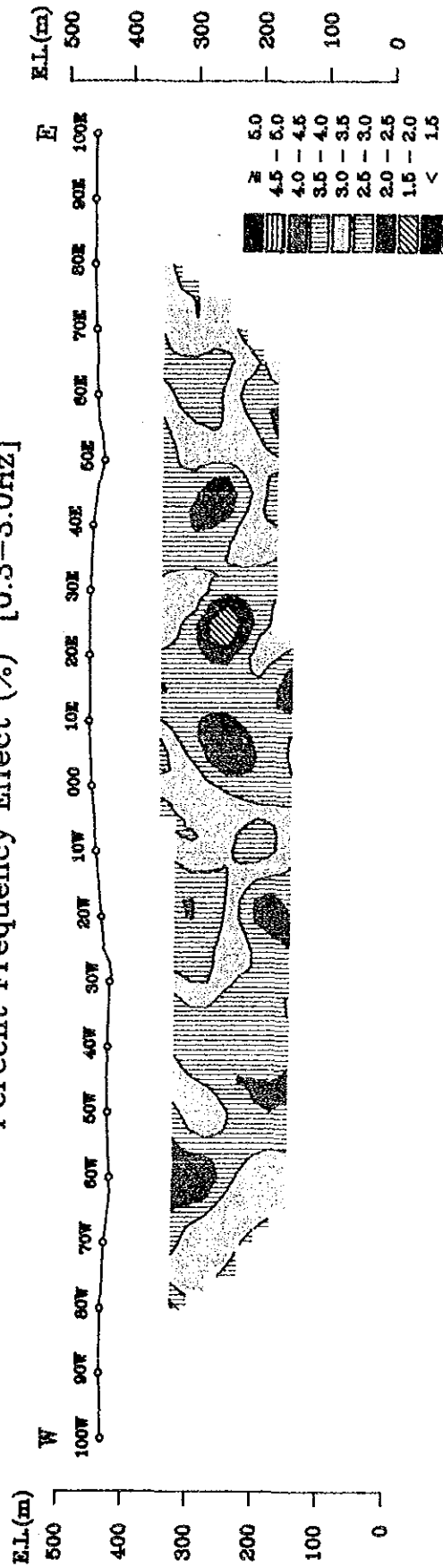
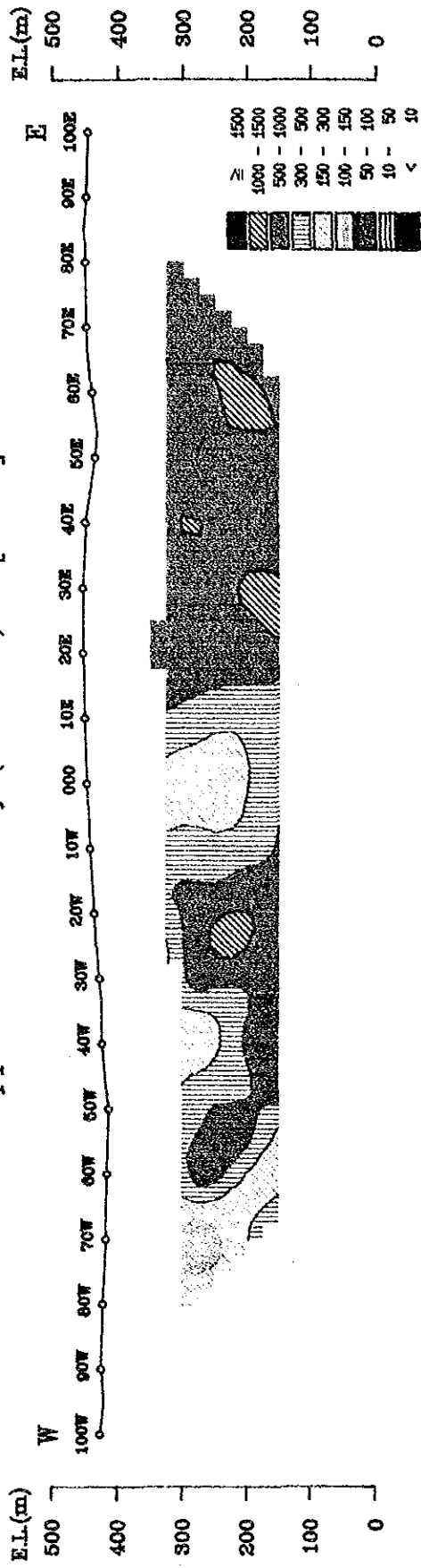


Fig. II-2-10 IP Pseudo-Section (Line-1390S)



# Line-1420S

## Apparent Resistivity (Ohm-m) [0.3Hz]



## Percent Frequency Effect (%) [0.3-3.0Hz]

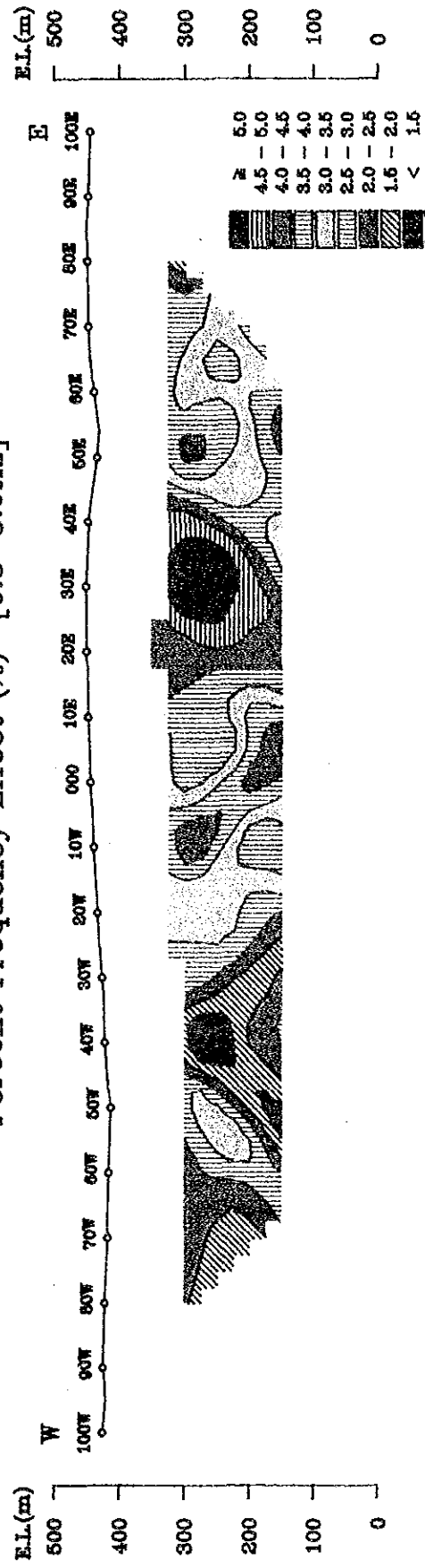
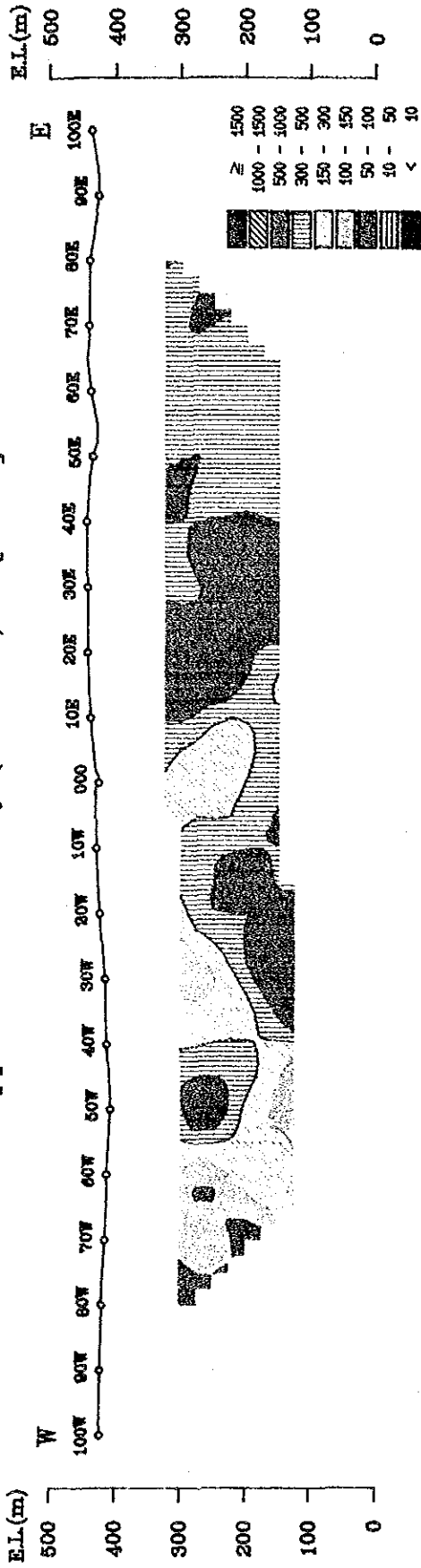


Fig. II-2-11 IP Pseudo-Section (Line-1420S)



# Line-1440S

## Apparent Resistivity (Ohm-m) [0.3Hz]



## Percent Frequency Effect (%) [0.3-3.0Hz]

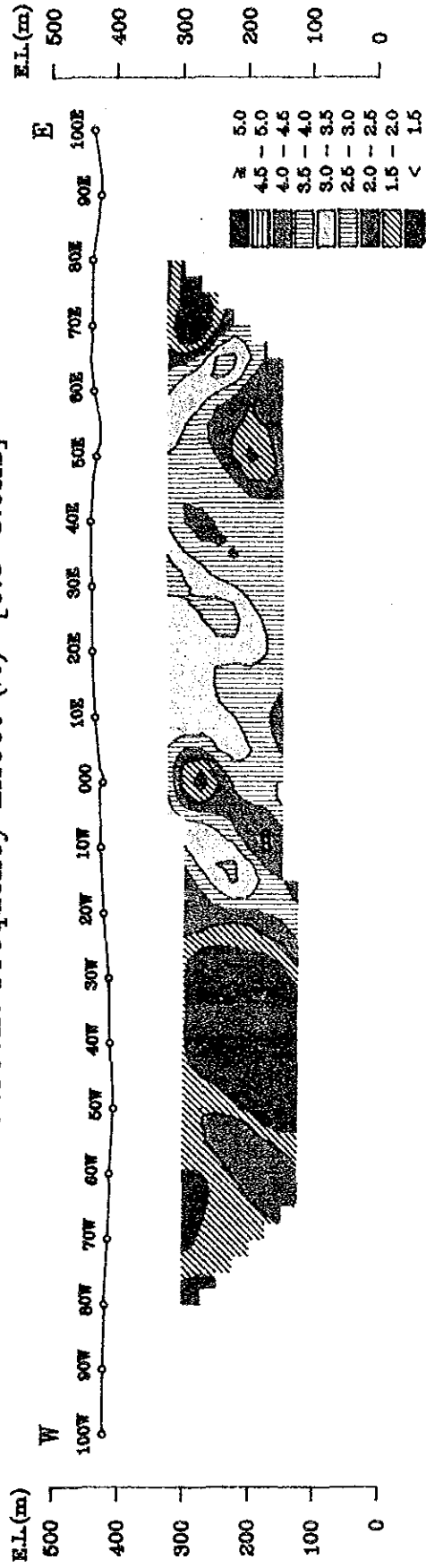


Fig. II-2-12 IP Pseudo-Section (Line-1440S)



### (1) n=1 Plan Maps

Apparent resistivities are clearly separated into high and low zones. The iso-apparent resistivity lines trending in the NE-SW direction and in the NE-SW and NW-SE directions are dominated in the eastern part and in the western part of the survey area, respectively, suggesting the existence of the geotectonic lines trending in each direction.

High apparent resistivities are found in the eastern, central and western parts of the survey area. Those in the western and eastern parts are of small-scale. The formers are distributed between measuring points 50W and 60W of the lines 1360S through 1375S, and the latter between 60E and 70E of the lines 1375S through 1390S. Those in the central part show the distribution pattern trending in N-S direction at the north of the line 1390S, and increase those distribution area toward the north. The increase of distribution area toward the north is halted near the fault structure trending in NNE-SSW direction presumed at measuring points 00 through 20W of the line 1330S, but, at the north beyond the fault structure those seem to extend toward the north, because according to the geologic map the  $Pip_4 vxt_2$  formation, causing high apparent resistivity, extends toward north and from the results of the second-phase SIP survey, it was suggested that those observed in the second phase extend toward the south.

Low apparent resistivities are widely distributed in the southern, northwestern, eastern and southeastern parts of the area. Those in the southern part are observed at the west of measuring point 00 of the lines 1390S through 1450S, and extend to those in the northwestern part. Those in the eastern and southeastern parts show the notable distribution pattern trending in NNE-SSW direction, suggesting the existence of the fault structures and/or geologic boundaries.

IP anomalies with PFE of more than 3.0% are mainly found within the medium-to-high apparent resistivity zones, showing the distribution patterns of "U" shapes. These patterns correspond to the strikes of the probable fault structures.

### (2) n=3 Plan Maps

Medium-to-high apparent resistivities are distributed from a northern part to the central part of the survey area and low apparent resistivities are concentrated in the southern part of the survey area.

High apparent resistivities in this map are found in a wider area than those in the plan map for n=1, that is, those are distributed broadly at the north of the line 1450S. This distribution suggests that the weathering does not affect toward the depth and the compactness and the content of quartz in schist increase toward the depth.



Low apparent resistivities are distributed at the three parts of the southern portion of the survey area, being separated by medium apparent resistivities, and each of those extends toward the south beyond the survey area. Those trending in NNE-SSW direction, observed in the distribution area of medium apparent resistivities in the plan map of  $n=1$ , are diminished.

The distributions of IP anomalies are grouped into the following three zones:

- 1) IP anomalous zone trending in N-S direction at the central part of the survey area.
- 2) IP anomalous zone trending in NE-SW direction at the southeastern part.
- 3) IP anomalous zone trending in N-S direction at the southern part.

Among these three IP anomalous zones, the first two zones seem to be due to the same IP anomalous sources, because the both zones form a single IP anomalous zone in the plan map of  $n=1$ . While, the zone of the item 3) seems to be a local IP anomaly caused by the anomalous source distributed around the depth of 200 m G. L.

### (3) $n=5$ Plan Maps

On this map, apparent resistivities vary from the high to the low towards the south. High apparent resistivities are widely distributed at the central part through the northern part of the survey area. Low-to-medium apparent resistivities are concentrated at the southern part and are observed at the western and eastern edges, and in the direction of N-S at the central part, showing the distribution pattern of "W" shape which encloses the above high apparent resistivities.

Two IP anomalous zones of the PFE of more than 3.0% are distributed at the central part through the western part, and at the southwestern part of the area.

The former IP anomalous zone, in which the MBP-4 hole was drilled, shows the trend of N-S direction, and is distributed within high apparent resistivities mainly and within low-to-medium apparent resistivities at the southern edge of the zone.

The latter zone shows the distribution pattern of ellipsoidal shape different from the ones on the plan maps of  $n=1$  and 3, and is found in a distribution area of medium apparent resistivities. On the plan maps of  $n=1$  and 3, this zone shows the trend in NNE-SSW direction clearly, and the P.F.E. of more than 4.0% thought as a center of the anomalous zone is found only at one portion. However, on this depth level, the four centers of the zone are found 1) between the lines 1375S (between measuring points 20E and 30E) and 1390S (between 40E and 50E), 2) between 1450S (between 20E and 30E) and 1430S (between 20E and 30E), 3) between 50E and 60E of the line 1420S and 4) between 40E and 50E of the line 1430S. Those at the first two locations are distributed in N-S direction and these directions were not observed in the plan maps of  $n=1$



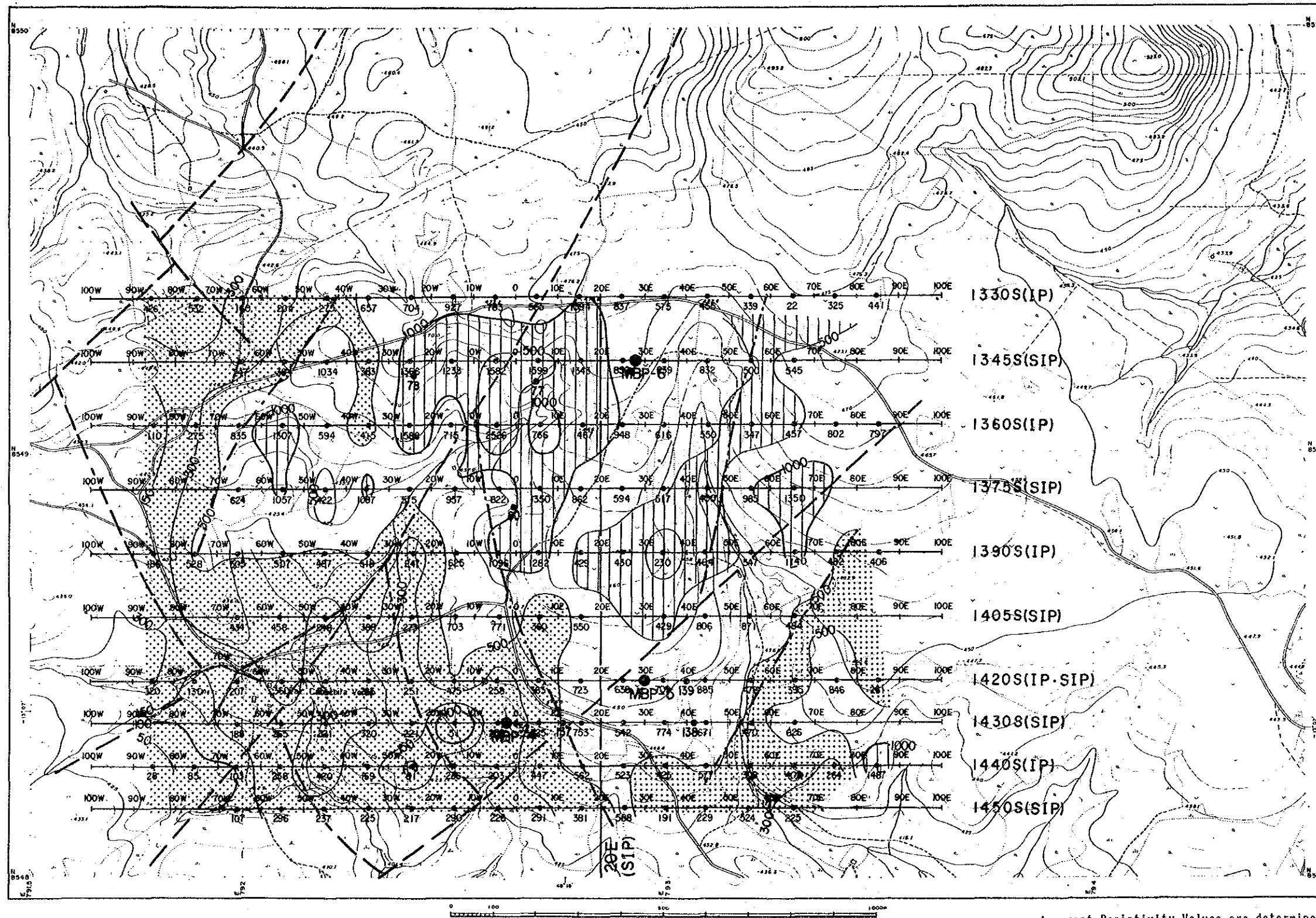


Fig. II-2-13 Apparent Resistivity Map [n-spread 1]

Apparent Resistivity Values are determined from the frequency of 0.375Hz for SIP, and from the frequency of 0.3Hz for IP



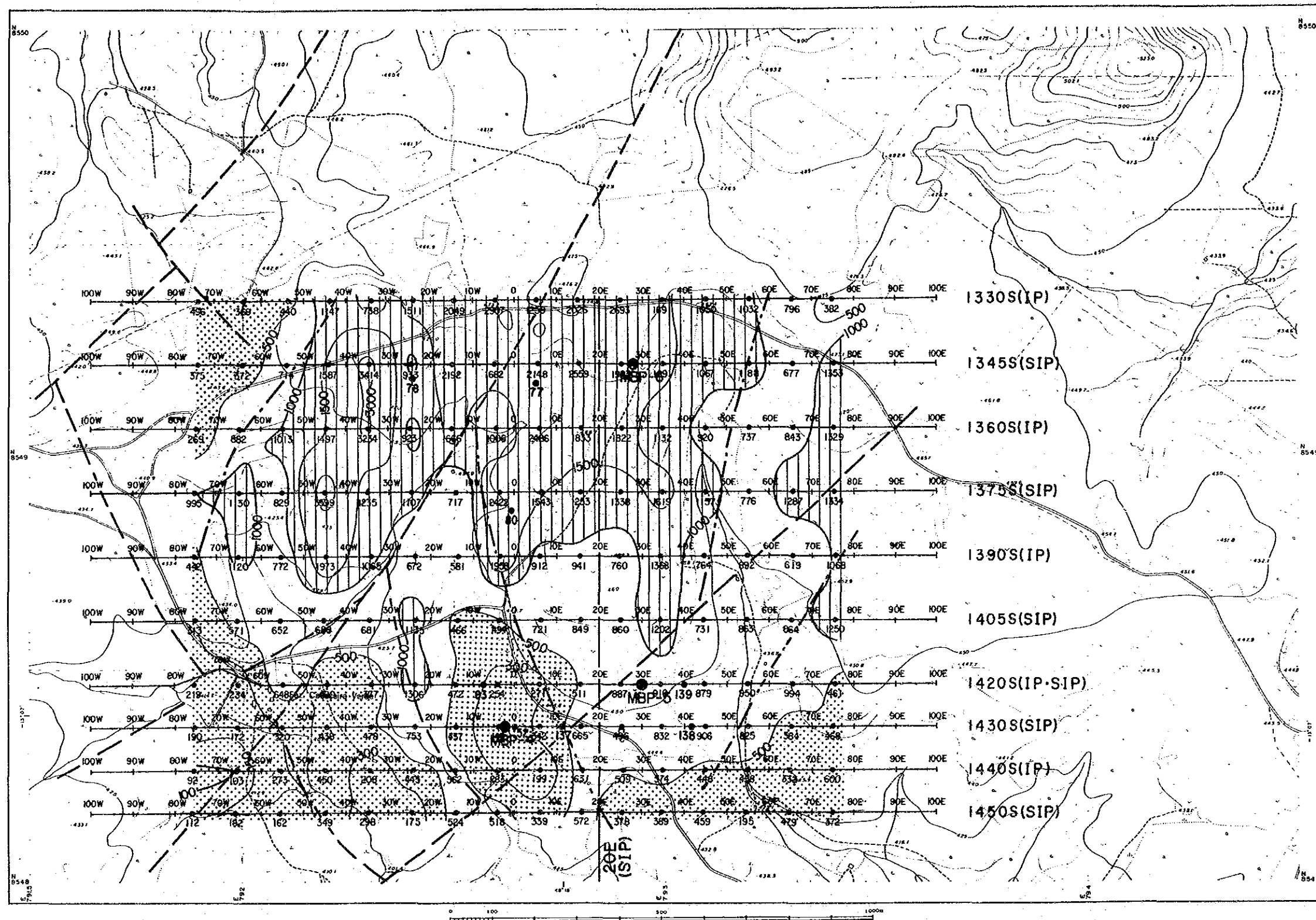
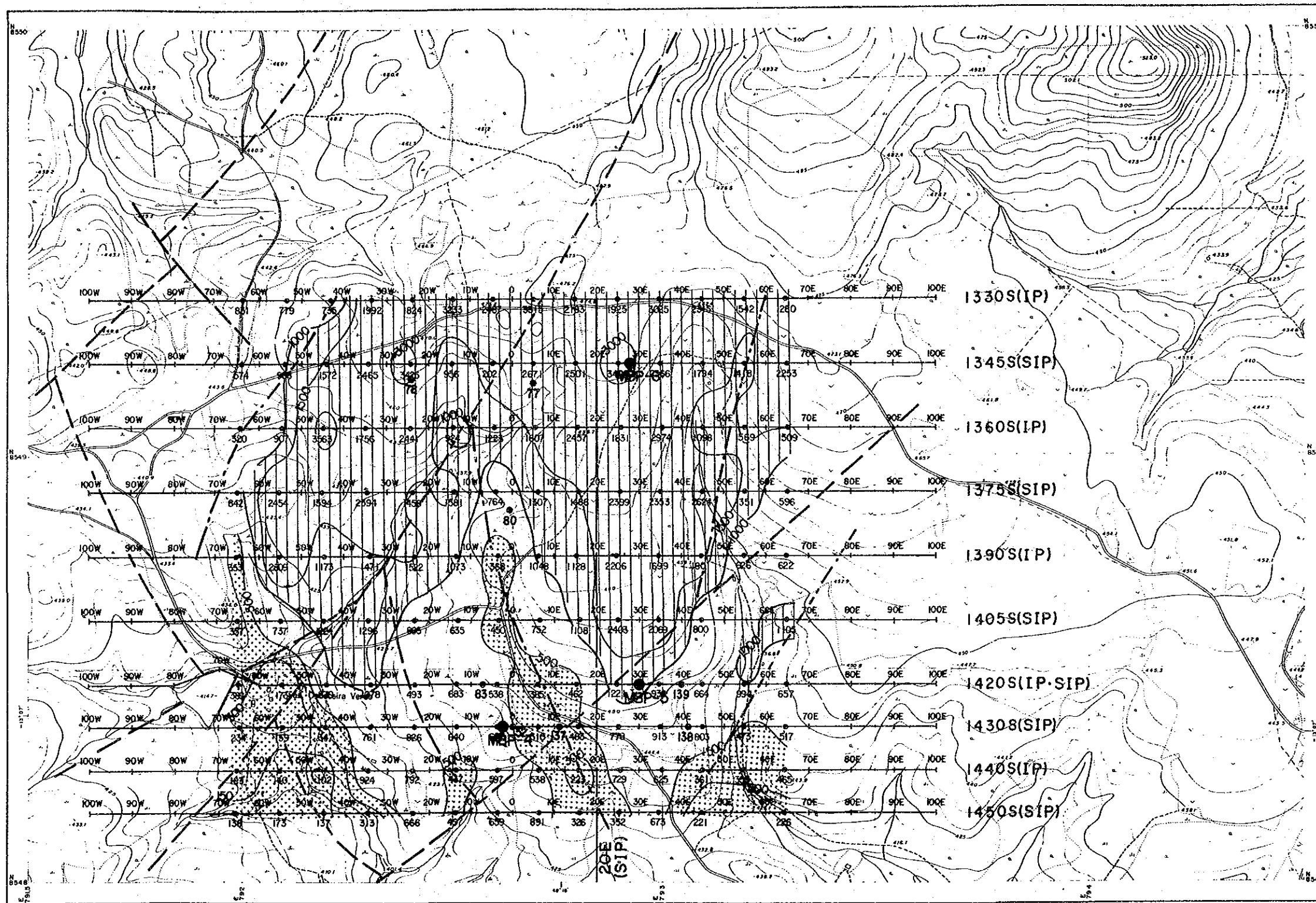


Fig. II-2-14 Apparent Resistivity Map [n-spread 3]

Apparent Resistivity Values are determined from the frequency of 0.375Hz for SIP, and from the frequency of 0.3Hz for IP





- LEGEND**
- SIP and IP Line
  - Drilling Point of MMAJ
  - Drilling Point of CPRM
  - ▨ 500 ≥ Rho Ωm
  - ▧ 1000 < Rho Ωm
  - - - Fault
  - · - · - Tectonic Line Inferred by Geophysical Survey

Apparent Resistivity Values are determined from the frequency of 0.375Hz for SIP, and from the frequency of 0.3Hz for IP

Fig. II-2-15 Apparent Resistivity Map [n-spread 5]





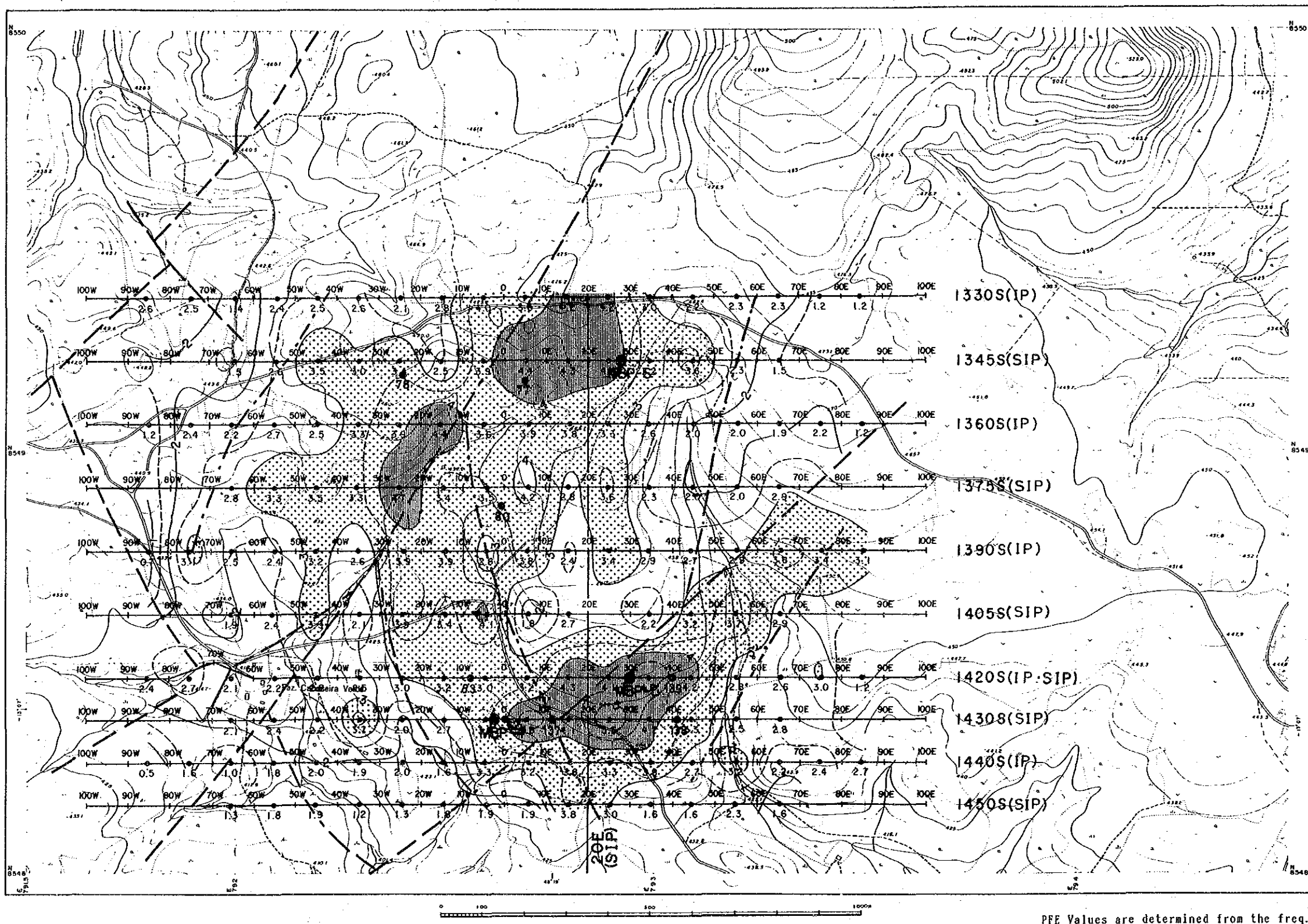


Fig. II-2-16 Frequency Effect Map [n-spread 1]

PFE Values are determined from the freq. of 0.375Hz~3.0Hz for SIP, and from the freq. of 0.3Hz~3.0Hz for IP



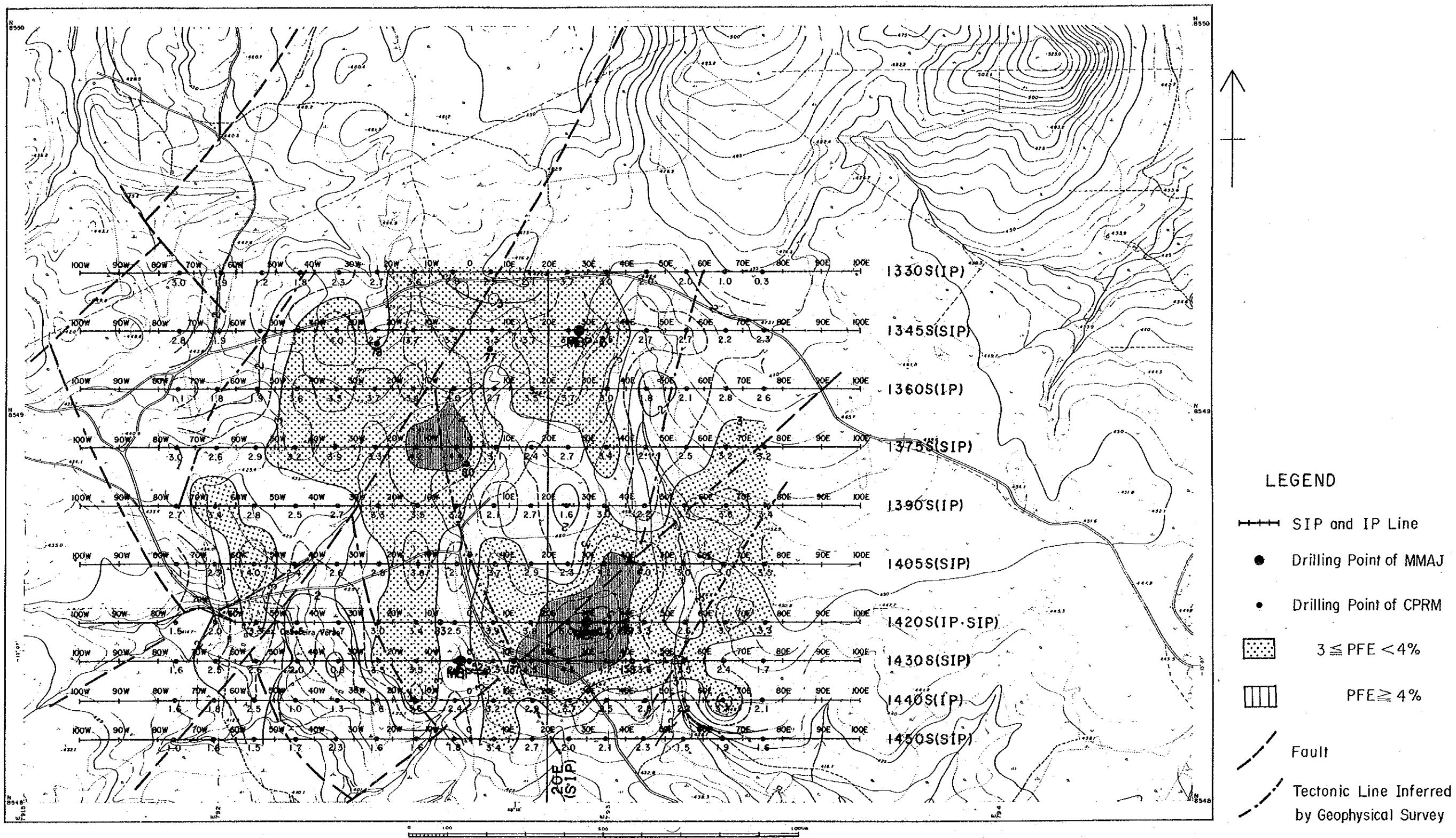
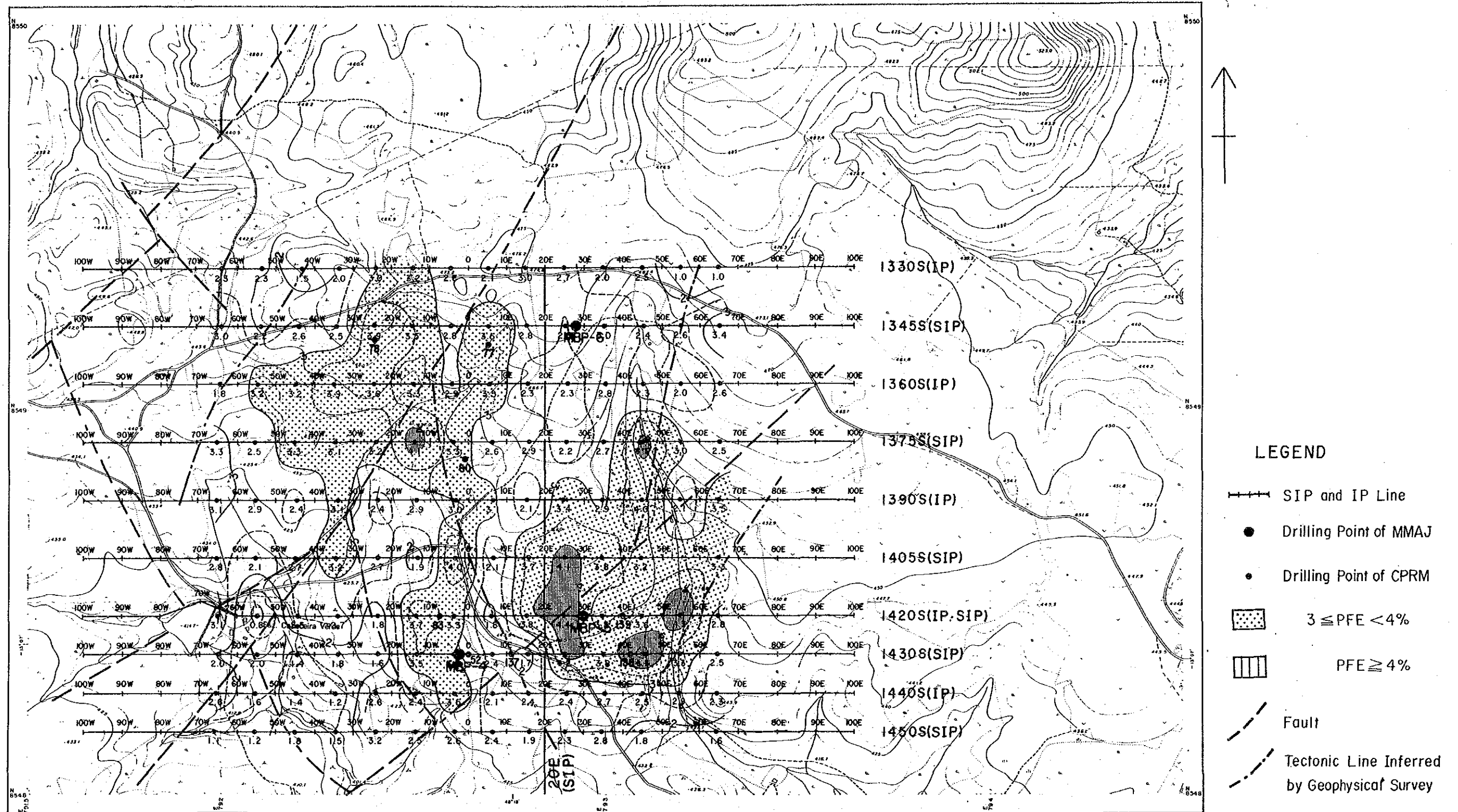


Fig. II-2-17 Frequency Effect Map [n-spread 3]

PFE Values are determined from the freq. of 0.375Hz~3.0Hz for SIP, and from the freq. of 0.3Hz~3.0Hz for IP





PFE Values are determined from the freq. of 0.375Hz~3.0Hz for SIP, and from the freq. of 0.3Hz~3.0Hz for IP

Fig. II-2-18 Frequency Effect Map [n-spread 5]

